

MACHINABILITY OF CARBON FIBER REINFORCED POLYMER (CFRP) COMPOSITES:
MODELING AND OPTIMIZATION USING TAGUCHI ANALYSIS AND MULTI-
OBJECTIVE GENETIC ALGORITHM

A Thesis

by

S M ABDUR ROB

Submitted to the graduate college of
The University of Texas Rio Grande Valley
In partial fulfillment of the requirements for the degree of

MASTER OF SCIENCE IN ENGINEERING

August 2021

Major: Manufacturing Engineering

MACHINABILITY OF CARBON FIBER REINFORCED POLYMER (CFRP) COMPOSITES:
MODELING AND OPTIMIZATION USING TAGUCHI ANALYSIS AND MULTI-
OBJECTIVE GENETIC ALGORITHM

A Thesis
by
S M ABDUR ROB

COMMITTEE MEMBERS

Dr. Anil Srivastava
Chair of Committee

Dr. Jianzhi Li
Committee Member

Dr. Rajiv Nambiar
Committee Member

Dr. Kye Hwan (Kevin) Lee
Committee Member

August 2021

Copyright 2021 S M Abdur Rob

All rights reserved

ABSTRACT

Rob, S M Abdur, Machinability of Carbon Fiber Reinforced Polymer (CFRP) Composites: Modeling and Optimization using Taguchi Analysis and Multi-Objective Genetic Algorithm.

Master of Science in Engineering, August, 2021, 83 pp., 30 tables, 59 figures, 41 references.

Carbon Fiber Reinforced Polymer (CFRP) composites have been widely used in aerospace, automotive, nuclear, and biomedical industries due to their high strength to weight ratio, corrosion resistant, durability and excellent thermo-mechanical properties in non-oxidative atmospheres. Machining of CFRP composites has always been a challenge for the manufacturers. In this study, turning operation has been performed on CFRP composites to investigate the effects of cutting parameters namely cutting speed, feed rate and depth of cut on the output characteristics including cutting force, surface roughness and tool wear using Taguchi Analysis. Regression Analysis has been used to develop mathematical models for cutting force, surface roughness and tool wear as a function of cutting speed, feed rate and depth of cut. A comparative study has been performed between coated and uncoated carbide inserts based on the optimal parameters in multi-objective optimization of cutting force, tool wear and surface roughness using Multi-Objective Genetic Algorithm (MOGA) during turning of CFRP composites in a CNC lathe machine. It was found that coated carbide inserts currently used, provide lower tool wear and surface roughness, but higher cutting forces compared to those of uncoated carbide inserts during turning of CFRP composites. The feed rate has been found as the most significant

parameters in turning of CFRP composites to minimize cutting force, tool wear and surface roughness. Cutting speed has been found more significant in tool wear when using uncoated carbide inserts.

DEDICATION

I want to dedicate my work to my parents Most Morzina Begum and Md Abu Sayed. My heartiest gratitude to the Almighty for making this difficult task easier for me through his continuous support. Without the constant guidance and help of my supervisor, family and friends, my journey at UTRGV would not have been successful.

ACKNOWLEDGMENTS

I would like to express my immense gratitude to my supervisor Dr Anil K. Srivastava for his continuous guidance and support. His expertise in advanced machining area and proper directions has helped me a lot to overcome all the difficulties successfully during my master's program at UTRGV. I feel grateful to him for giving me the opportunity to work in the Advanced Machining Laboratory under his close supervision. I am very thankful to my colleague Al Mazedur Rahman who has helped me a lot to understand the CNC machining process clearly within very short period of time. I want to thank my wife Roma Khanam for her continuous encouragement and motivation. I am thankful to Edgar Turribiates and Md Mofakkirul Islam for their help during my experimental works at Advanced Machining Laboratory.

TABLE OF CONTENTS

	Page
ABSTRACT.....	iii
DEDICATION.....	v
ACKNOWLEDGMENTS.....	vi
TABLE OF CONTENTS.....	vii
LIST OF TABLES.....	ix
LIST OF FIGURES.....	xii
CHAPTER I. INTRODUCTION.....	1
CHAPTER II. LITERATURE REVIEW.....	4
Performance Study of CFRP Turning Process.....	4
Optimization.....	6
Modeling.....	8
CHAPTER III. OBJECTIVES & METHODOLOGY.....	10
Objectives.....	10
Methodology.....	11
Experimentation.....	17
CHAPTER IV. RESULTS & DISCUSSION.....	22
Experimental Data.....	22
Taguchi Analysis: Effects of Machining Parameters on Turning Performance	
Characteristics.....	23

Linear Regression Model	53
Multi-objective Optimization using Multi-Objective Genetic Algorithm (MOGA).....	58
Validation for Multi-Objective Optimization.....	70
Comparative Study of the Machining Parameters between Coated and Uncoated Carbides	71
CHAPTER V. CONCLUSIONS	77
REFERENCES	79
BIOGRAPHICAL SKETCH	83

LIST OF TABLES

	Page
Table 1: Input factors and corresponding levels	11
Table 2: DOE using Taguchi L ₉ orthogonal array	11
Table 3: Cutting tool and workpiece specifications.....	19
Table 4: Taguchi L ₉ orthogonal array and the observed response values using coated carbide inserts	22
Table 5: Taguchi L ₉ orthogonal array and the observed response values using uncoated carbide inserts	23
Table 6: Response table for means of Cutting force (Coated Carbides).....	24
Table 7: Response table for signal to noise (S/N) ratios of Cutting force (Coated Carbides)	28
Table 8: Response table for means of Surface roughness (Coated Carbides)	29
Table 9: Response table for signal to noise (S/N) ratios of Surface roughness (Coated Carbides)	33
Table 10: Response table for means of tool wear (coated carbides).....	35
Table 11: Response table for signal to noise (S/N) ratios of tool wear (Coated Carbides)	38
Table 12: Response table for means of Cutting force (Uncoated Carbides).....	39

Table 13: Response table for signal to noise (S/N) ratio of cutting force (Uncoated Carbides)	42
Table 14: Response table of means of surface roughness (Uncoated Carbides)	44
Table 15: Response table for signal to noise (S/N) ratio of surface roughness (Uncoated Carbides)	48
Table 16: Response table of means of tool wear (Uncoated Carbides)	49
Table 17: Response table for signal to noise ratio (S/N) of tool wear (Uncoated Carbides)	52
Table 18: Parameters for GA	58
Table 19: Paretian points obtained from multi-objective optimization of cutting force and surface roughness (Coated Carbides).....	59
Table 20: Paretian points obtained from multi-objective optimization of cutting force and tool wear (Coated Carbides)	61
Table 21: Pareto optimal solution obtained from multi-objective optimization of surface roughness and tool wear (Coated Carbides).....	62
Table 22: Pareto optimal solution obtained from multi-objective optimization of cutting force, surface roughness and tool wear (Coated Carbides)	63
Table 23: Pareto optimal solutions obtained from multi-objective optimization of cutting force and surface roughness (Uncoated Carbides)	65
Table 24: Pareto optimal solutions obtained from multi-objective optimization of cutting force and tool wear (Uncoated Carbides)	67
Table 25: Pareto optimal solution obtained from multi-objective optimization of surface roughness and tool wear (Uncoated Carbides).....	68

Table 26: Pareto optimal solution obtained from multi-objective optimization of cutting force, surface roughness and tool wear (Uncoated Carbides)	69
Table 27: Validation experiment results for the optimal machining parameters using Coated Carbides	70
Table 28: Validation experiment results for the optimal machining parameters using uncoated carbides	71
Table 29: Most significant machining parameters for coated and uncoated carbides	73
Table 30: Optimal machining parameters for coated and uncoated carbide inserts during turning of CFRP composites	74

LIST OF FIGURES

	Page
Figure 1: Multi-Objective Genetic Algorithm implementation process	15
Figure 2: Cutting tool (Coated Carbide)	18
Figure 3: Work piece	18
Figure 4: Cutting force measurement set up using Kistler 9255C Dynamometer	19
Figure 5: Tool wear measurement set up using VHX-5000 Optical Microscope.....	20
Figure 6: Surface roughness measurement set up using MahrSurf M 300 C profilometer.....	20
Figure 7: Schematic diagram of experimental setup.....	21
Figure 8: Tool path and cutting force direction	21
Figure 9: Effects of machining parameters on cutting force (Coated Carbides)	25
Figure 10: Contour plot for cutting force: cutting speed vs feed rate (Coated Carbides)	26
Figure 11: Contour plot for cutting force: cutting speed vs depth of cut (Coated Carbides)	26
Figure 12: Contour plot for cutting force: feed rate vs depth of cut (Coated Carbides)	27
Figure 13: Main effect plot of S/N ratios for cutting force (Coated Carbides).....	28
Figure 14: Effects of machining parameters on surface roughness (Coated Carbides)	30

Figure 15: Optical microscopic view of machined surface obtained at cutting speed of 100 m/min, feed rate of 0.05 mm/rev and depth of cut 0.15 mm	31
Figure 16: Contour plot for surface roughness: cutting speed vs feed rate (Coated Carbides)	31
Figure 17: Contour plot for surface roughness: Cutting speed vs depth of cut (Coated Carbides)	32
Figure 18: Contour plot for surface roughness: Feed rate vs depth of cut (Coated Carbides)	32
Figure 19: Main effect plots for S/N ratios of surface roughness (Coated Carbides).....	34
Figure 20: Effect of machining parameters on tool wear (Coated Carbides)	35
Figure 21: Contour plot for tool wear: cutting speed vs feed rate (Coated Carbides)	36
Figure 22: Contour plot for tool wear: cutting speed vs depth of cut (Coated Carbides)	36
Figure 23: Contour plot for tool wear: feed rate vs depth of cut (Coated Carbides)	37
Figure 24: Main effect plots for S/N ratios of tool wear (Coated Carbides)	38
Figure 25: Effects of machining parameters on cutting force (Uncoated Carbides)	40
Figure 26: Contour plot for cutting force: cutting speed vs feed rate (Uncoated Carbides)	40
Figure 27: Contour plot for cutting force: cutting speed vs depth of cut (Uncoated Carbides)	41
Figure 28: Contour plot for cutting force: feed rate vs depth of cut (Uncoated Carbides)	41
Figure 29: Main effects plot for S/N ratio of cutting force (Uncoated Carbides).....	43

Figure 30: Effects of machining parameters on surface roughness	
(Uncoated Carbides)	45
Figure 31: Powder like chips produced during turning process of CFRP	45
Figure 32: Contour plot for surface roughness: Cutting speed vs feed rate	
(Uncoated Carbides)	46
Figure 33: Contour plot for surface roughness: Cutting speed vs depth of cut	
(Uncoated Carbides)	47
Figure 34: Contour plot for surface roughness: Feed rate vs depth of cut	
(Uncoated Carbides)	47
Figure 35: Main effect plots for S/N ratio of surface roughness (Uncoated Carbides)	48
Figure 36: Effects of machining parameters on tool wear (Uncoated Carbides).....	50
Figure 37: Contour plot for tool wear: Cutting speed vs feed rate	
(Uncoated Carbides)	50
Figure 38: Contour plot for tool wear: Cutting speed vs depth of cut	
(Uncoated Carbides)	51
Figure 39: Contour plot for tool wear: Feed rate vs depth of cut (Uncoated Carbides)	51
Figure 40: Main effects plot for S/N ratio of tool wear (Uncoated Carbides).....	53
Figure 41: Normal probability plot of residuals for cutting force (Coated Carbides)	54
Figure 42: Normal probability plot of residuals for surface roughness	
(Coated Carbides)	55
Figure 43: Normal probability plot of residuals for tool wear (Coated Carbides).....	55
Figure 44: Normal probability plot of residuals for cutting force (Uncoated Carbides)	56

Figure 45: Normal probability plot of residuals for surface roughness (Uncoated Carbides)	57
Figure 46: Normal probability plot of residuals for tool wear (Uncoated Carbides).....	57
Figure 47: Pareto front of cutting force and surface roughness (Coated Carbides).....	60
Figure 48: Pareto front of cutting force and tool wear (Coated Carbides)	62
Figure 49: Pareto front of cutting force, surface roughness and tool wear (Coated Carbides)	64
Figure 50: Pareto front of cutting force and surface roughness (Uncoated Carbides).....	66
Figure 51: Pareto front of cutting force and tool wear (Uncoated Carbides)	68
Figure 52: Pareto front of cutting force, surface roughness and tool wear (Uncoated Carbides)	70
Figure 53: Comparative study on the effects of machining parameters on cutting force between coated and uncoated carbide inserts based on Taguchi Analysis	72
Figure 54: Comparative study on the effects of machining parameters on surface roughness between coated and uncoated carbide inserts based on Taguchi Analysis	72
Figure 55: Comparative study on the effects of machining parameters on tool wear between coated and uncoated carbide inserts based on Taguchi Analysis	73
Figure 56: Comparative study on optimal parameters between coated and uncoated carbide inserts to minimize cutting force and surface roughness	75
Figure 57: Comparative study on optimal parameters between coated and uncoated carbide inserts to minimize cutting force and tool wear	76
Figure 58: Comparative study on optimal parameters between coated and uncoated carbide inserts to minimize surface roughness and tool wear.....	76

Figure 59: Comparative study on optimal parameters between coated and uncoated carbide inserts to minimize cutting force, surface roughness and tool wear 76

CHAPTER I

INTRODUCTION

Fiber-reinforced composite materials consist of fibers of high strength and modulus embedded in or bonded to a matrix with distinct interfaces (boundaries) between them. In general, fibers are the principal load-carrying members, while the surrounding matrix keeps them in the desired location and orientation, acts as a load transfer medium between them, and protects them from environmental damages (Mallick, 1993). Carbon fiber reinforced polymer (CFRP) composites are widely used in aerospace, aeronautical, automotive, nuclear and biomedical industries due to their high strength to weight ratio, corrosion resistance, durability, excellent thermo-mechanical properties in non-oxidative atmospheres, high chemical inertness and good biocompatibility with the human body (Ferreira et al., 2001; Roy et al.; Savage, 2012).

Though composites are preferred to be manufactured to near net shape due to their inherent machinability problems, processes like turning, milling and drilling are unavoidable in order to improve the surface finish, provide easy mounting and joining surfaces (Kim et al., 1992). Machining of CFRP has been a great challenge for the manufacturers due to its nonlinear, inhomogeneous, and abrasive properties. Traditional machining of CFRP faces some problems including high cutting forces, high torque, high surface roughness, severe delamination, high tool wear, high cutting temperature, etc.(Sasahara et al., 2014; Soo et al., 2012). Dandekar & Shin

reviewed the machining of composite materials and found that the most important parameter of cutting force, surface quality and tool wear during machining of fiber reinforced composites are fiber orientation, tool geometry and machining parameters (Dandekar & Shin, 2012).

There are various empirical modeling techniques that can be applied for machining applications such as Linear Regression Modeling, Artificial Neural Network (ANN), polynomial and fuzzy modeling along with process optimization through Taguchi, Response Surface Methodology and Genetic Algorithm (Dureja et al., 2016). Linear regression model is the simplest modeling technique where higher R^2 value indicates that the model strongly represents the relationship between input parameters and the output responses. Artificial Neural Network and Fuzzy Modeling are widely used to simulate the machining performances. Response Surface Methodology has been used extensively in the literature to develop predictive models for different machining characteristics. Genetic Algorithm has also been used widely in the previous literature for modeling and multi-response optimization during turning process. Taguchi method has been widely used for design of experiments (DOE) in machining operations because it helps to reduce the number of experiments without increasing significant error, thus saving time for experiments and over-all cost.

In general, machining of fiber reinforced composite materials is very expensive process. So, optimization of cutting parameters is very important in machining of composites to ensure quality of the machined parts, reduce the machining cost and to increase the machining effectiveness (D'addona & Teti, 2013). The cutting parameters are often selected based on the experience or by recommendations of cutting tools' manufacturers. Their selection influences on tool life, machining time and cost of manufacturing (Petkovic & Radovanovic, 2013). Optimization of cutting parameters is usually difficult task (Jain & Jain, 2000), where the

following aspects are required: knowledge of machining, empirical equations relating the tool life, forces, power, surface finish, etc., to develop realistic constraints, specification of machine tool capabilities, development of an effective optimization criterion and knowledge of mathematical and numerical optimization techniques (Sönmez et al., 1999).

Turning of Carbon Fiber Reinforced Polymer (CFRP) composites involves with a lot of challenges such as fiber delamination, tool wear, cutting force, surface roughness etc. Due to extensive abrasiveness, tool wear is very high during turning of CFRP. Fiber delamination is another major problem in CFRP machining which can affect the tool wear and surface finish as well. Fiber orientation and the tool edge angle can also significantly impact the tool life and surface finish. All the response characteristics such as cutting force, tool wear and surface roughness depend largely on the variation of cutting parameters during turning process. So, finding the best combination of machining parameters such as cutting speed, feed rate and depth of cut is a major concern while turning the CFRP composites.

In this thesis, an extensive investigation has been performed on the turning of CFRP composites with the variation of different cutting parameters and the corresponding output characteristics have been studied using statistical analysis tools. Taguchi design of experiments has been used to complete the experimental design where Taguchi L₉ orthogonal array has been used to perform the experiments. S/N Analysis has been used to investigate the effects of machining parameters on response characteristics and Linear Regression Analysis has been used to develop the mathematical models for response characteristics. Multi-Objective Genetic Algorithm has been applied to find the optimal machining parameters to minimize cutting force, surface roughness and tool wear.

CHAPTER II

LITERATURE REVIEW

Machining characteristics of CFRP composites has been studied from various perspective by the previous researchers. Machining system consists of cutting tool, workpiece, cutting mechanism as well as material removal process which need to be investigated to improve the machining performance. Analysis of the effects of cutting parameters such as cutting speed, feed rate, depth of cut, tool geometry and tool approaching angle on the output characteristics such as cutting force, surface roughness, tool wear, tool tip temperature and material removal rate have been studied by the previous researchers. Modeling of the machining characteristics has also been performed to predict the effect of machining parameters on the desired output characteristics. Researchers have tried to optimize the machining condition using different approaches to reduce the overall production cost during machining of CFRP composites. Following sections provide a review of the previous research activities on the turning of CFRP composites.

Performance Study of CFRP Turning Process

Several researchers have studied the performance of different tool materials and tool geometry during turning of CFRP composites. Ferreira et al. (Ferreira et al., 1999) studied the performance of different tool materials such as ceramics, cemented carbide, cubic boron nitride

(CBN), and Poly-crystalline diamond (PCD) during turning of CFRP composites and found that PCD cutting tools are best suited to the finish turning of CFRP. The researchers concluded that the fiber orientation, matrix content and fiber type have significant impacts on the machinability of CFRP composites. Rahman et. al. (Rahman et al., 1999) studied the machinability of CFRP using different cutting tool inserts namely, uncoated tungsten carbides, ceramic and cubic boron nitride (CBN) varying machining parameters and made comparison among the cutting inserts based on the chip formation, tool wear, surface roughness and relative performance of different inserts.

Rajasekaran et al. (Rajasekaran, Palanikumar, et al., 2013; Rajasekaran et al., 2012b) studied the influence of cutting parameters on surface roughness during turning of CFRP composites using ceramic cutting tool. They reported that the most influencing cutting parameters on surface roughness is the feed rate because surface roughness increases with the increase of feed rate, but they also found that surface roughness tends to get improved with the increase of cutting speed. They also studied the influence of cutting parameters on surface roughness during turning of CFRP composites using CBN cutting tool and reported that surface roughness increases with the increase of feed rate but decreases with the increase of cutting speed. So, a combination of lower feed rate and higher cutting speed can result in an improved surface finish. However, depth of cut was found insignificant for surface finish during turning of CFRP composites.

Sauer et. al. (Sauer et al., 2020) performed turning and orthogonal turn-milling of CFRP and compared the results based on process forces and achievable shape and surface quality. The researchers identified a strong relation between cutting force and the cross-section of undeformed chip. Chang et. al. (Chang & Chang, 2011) investigated the temperature of carbide

tip's surface during turning of CFRP using sharp worn main cutting-edge tool. They developed a finite element model for tool tip's surface temperature during oblique cutting of CFRP in turning process.

In another experiment, Chang (Chang, 2015) used nine types of chamfered main cutting-edge nose radius tools during turning of CFRP composites and developed a cutting temperature model to study the cutting temperature of tip's surface with the variations of shear and friction plane areas occurring in tool nose situations. Demir et. al. (Demir & Adiyaman, 2019) studied the effects of tool approaching angle, feed rate and spindle speed on the shape of the chip, length of fibers, surface roughness, and tool wear during turning of CFRP composites and reported that feed rate is the most influencing factor during turning of CFRP followed by tool approach angle and spindle speed.

Optimization

Several researchers have studied the process optimization during turning of CFRP using different objective functions and optimization techniques (D'addona & Teti, 2013; Datta & Majumder, 2010; Petkovic & Radovanovic, 2013; Saravanakumar et al., 2012; Sardinas et al., 2006). Objective function may be to optimize a single objective such as the machining cost, production time, surface roughness and MRR or to optimize two conflicting issue such as machining time vs minimum production cost, operation time vs tool life etc. Various techniques are being used to optimize a problem. The techniques that have been used for optimization include Harmony Search (HS) algorithm (Abhishek et al., 2016), JAYA algorithm (Hari Mohan Pandey, 2016), Teaching Learning Based Optimization (TLBO) algorithm (Rao & Patel, 2013; Rao et al., 2012) and Imperialist Competitive Algorithm (ICA) (Abhishek, Kumar, et al., 2017a),

Genetic Algorithm (GA) (Datta & Majumder, 2010), fuzzy logic, scatter search technique, Taguchi technique and Response Surface Methodology.

Harmony Search (HS) algorithm is a meta-heuristic optimization algorithm which imitates the principles of improvisation process of musicians to find the best harmony for music. HS is one of the most popular optimization algorithms in the field of soft computing. Abhishek et al. (Abhishek et al., 2014) applied Harmony Search (HS) algorithm to optimize cutting force and surface roughness during turning of CFRP composites using HSS cutting tool and compared the results with those of Genetic Algorithm (GA). They compared HS with GA based on their effectiveness in minimizing surface roughness and resultant cutting forces and concluded that HS is more efficient than GA. Kumar et. al (Kumar & Sait, 2017) applied Taguchi's design of experiment, artificial neural network, and genetic algorithm to predict the cutting force and optimize the machining parameters during turning of CFRP composites using a carbide cutting tool.

JAYA algorithm is a global optimization algorithm which can be used to optimize both constraint and unconstrained problem using only a few numbers of control parameters such as maximum number of generations, population size, and number of design variables without requiring algorithm specific control parameters (H. M. Pandey, 2016). TLBO is a population-based optimization algorithm which imitates the teaching learning phenomenon of the teachers and learners in the classroom (Rao & Patel, 2013; Rao et al., 2012).

Abhishek et. al (Abhishek, Kumar, et al., 2017a) applied JAYA algorithm to optimize machining parameters using material removal rate (MRR), roughness average (Ra), and net cutting force as machining performance characteristics during turning of CFRP composites and compared the results with TLBO, GA, and ICA. They found a good consistency among the

results obtained from different algorithms. In another study, they optimized cutting parameters (cutting speed, feed rate and depth of cut) during turning of CFRP using TLBO algorithm with the machining performance characteristics as MRR, cutting force and surface roughness and compared the optimization results with those of GA (Abhishek, Kumar, et al., 2017b). They reported that TLBO is more efficient in optimizing machining parameters in comparison with GA during turning of CFRP composites.

In another experiment, Abhishek et al. (Abhishek, Datta, Masanta, et al., 2017) performed the optimization of machining parameters to improve surface roughness, MRR and to reduce cutting force during turning of CFRP using ICA (Imperialist Competitive Algorithm) and compared the results to that of GA. Abhishek et al. (Abhishek, Datta, & Mahapatra, 2017) optimized MRR, Surface Roughness, and Maximum Tool-Tip Temperature during turning of CFRP using Harmony Search (HS) algorithm and Teaching-Learning-Based Optimization (TLBO) algorithm. Ganesan et al. (Ganesan & Mohankumar, 2013) used Genetic Algorithm to perform multi-objective optimization to minimize the production cost, operation time and tool wear during turning of CFRP composites.

Modeling

Various models have been developed to predict the machining characteristics of CFRP composites. Researchers have focused to predict the cutting force, tool wear, tool tip temperature and surface roughness during turning of CFRP composites using different modeling technique such as Finite Element Modeling (FEM), fuzzy modeling etc. Finite Element Modeling (FEM) is a numerical method which is used to predict the performance characteristics of any physical systems where the system or component being studied is divided into discrete elements resulting in a finite element mesh and the equations developed for the individual system's characteristics

are assembled to develop the model for the entire system of component. Fuzzy modeling is mathematical technique to deal with the vagueness and imprecise information by applying fuzzy rules which are developed based on human experience and database.

Chang et al (Chang & Chang, 2011) proposed a finite element model to determine the surface temperature of carbide tool tip during turning of CFRP composites. In another experiment, Chang (Chang, 2015) used nine types of chamfered main cutting-edge nose radius tools during turning of CFRP and developed a cutting temperature model for the tip's surface of the tools with the variations of shear and friction plane areas occurring in tool nose situations. They compared the predicted temperature values with those of experimental values and found that predicted values are close to the experimental values.

Rajasekaran et al. (Rajasekaran, Gaitonde, et al., 2013) modeled and predicted the machining force and specific cutting pressure using fuzzy logic during turning of CFRP composites and found that the predicted values of responses such as machining forces and specific pressure are quite closer to the experimental values. In another study, Rajasekaran et al (Rajasekaran et al., 2012a) developed a fuzzy model to predict the cutting force during turning of CFRP using PCD cutting tool and observed that the developed model provides desired values of response characteristics while comparing with those of experimental values. Belmonte et al. (Belmonte et al., 2004) performed turning of CFRP composites using uncoated and CVD diamond coated Si_3N_4 cutting tools and investigated the cutting forces and tool wear as a function of cutting speed. They reported that CVD coated Si_3N_4 cutting tools show better performance compared to the uncoated Si_3N_4 cutting tools during turning of CFRP in terms of lower cutting force and lower tool wear.

CHAPTER III

OBJECTIVES & METHODOLOGY

Objectives

Literature search reveals that Multi-Objective optimization of cutting force, tool wear and surface roughness during turning of CFRP composites has not been performed in the previous literature. Moreover, a comparative study between the coated and uncoated carbide cutting tool based on the optimal cutting parameters need to be performed during turning of CFRP composites. Based on the literature survey and the subsequent research gaps, the objective of this study has been set to investigate the effects of machining parameters (cutting speed, feed rate and depth of cut) on cutting force, surface roughness and tool wear during turning of CFRP using coated and uncoated carbide cutting tools. The study is mainly focused on:

- Developing mathematical models for cutting force, surface roughness and tool wear as a function of cutting speed, feed rate and depth of cut applying linear regression analysis and using those models as fitness functions to perform the multi-objective optimization of machining parameters with Genetic Algorithm to minimize cutting force, tool wear and surface roughness.
- Performing a comparative study on the machining performance of coated and uncoated carbide cutting tool based on cutting force, tool wear and surface roughness during

turning of CFRP composites and analyzing the optimized machining parameters for coated and uncoated carbide cutting tools.

Methodology

Taguchi Design of Experiments

Taguchi Design of Experiments (DOE) uses an orthogonal array to design the experimental steps using different levels of machining parameters. In the present study, Taguchi L₉ orthogonal array has been used to design the experiments. There are three main machining parameters in turning of composites: cutting speed, feed rate and depth of cut. Each factor has three different levels. Tables 1 and 2 illustrate the factors and Taguchi Design of Experiments used in this study.

Table 1: Input factors and corresponding levels

Factors	Level 1	Level 2	Level 3
Cutting speed (m/min)	75	100	125
Feed rate (mm/rev)	0.05	0.075	0.1
Depth of cut (mm)	0.1	0.15	0.2

Table 2: DOE using Taguchi L₉ orthogonal array

Experiment	Level of factors		
	Cutting Speed	Feed rate	Depth of cut
1	1	1	1
2	1	2	2
3	1	3	3
4	2	1	2
5	2	2	3
6	2	3	1
7	3	1	3
8	3	2	1
9	3	3	2

Taguchi Analysis

In Taguchi analysis, response characteristics are classified into two categories- Signal and Noise. Signal is defined as the desirable effects and the Noise is defined as the undesirable effects of the response characteristics. Signal refers to the control factors and Noise refers to the uncontrollable factors. Taguchi analysis uses the Signal to Noise (S/N) ratio to identify the optimal control parameter setting which minimizes the effects of noise factors. The higher the value of S/N ratio, the lower the effect of noise factors on the response characteristics. There are three types of S/N ratios used in Taguchi Analysis- smaller the better, larger the better and nominal the best. Smaller the better S/N ratio is used to minimize the response characteristics while larger the better S/N ratio used to maximize the response characteristics. In this experiment, smaller the better S/N ratio has been used to minimize the cutting force, surface roughness and tool wear. Equation 1 is used to calculate the nominal the better S/N ratio-

$$S/N = -10 \log_{10} \left[\frac{1}{n} \left(\sum_{i=1}^n y_i^2 \right) \right] \quad (1)$$

Here, n is the total number of measurements in each experiment and y_i is the measurement value of i^{th} run. While using single performance characteristic, highest S/N ratio represents the optimal level of process parameter. On the other hand, while using multiple performance characteristics the overall evaluation of all the S/N ratios corresponding to each machining parameter is required.

Regression Analysis

Regression analysis is a set of statistical tools used to estimate the relationship between dependent (output characteristics) and independent (input parameters) variables. There are several types of regression analysis including linear regression, multiple linear regression, and

nonlinear regression. Linear regression is the most common type of regression analysis which provides a line using a specific mathematical standard that best fits all the data points obtained from an experimental result. The simple linear regression can be expressed as-

$$y = \alpha + \beta x + \varepsilon \quad (2)$$

Here, y is the dependent variable, α is the intercept, β is the slope, x is the independent variable and ε is the residual error. The goodness of fit for a linear regression model is determined using a goodness of fit measure value called R^2 . R^2 refers to the statistical measurement of how close the data values are to the fitted regression line. It is also known as the coefficient of determination, or the coefficient of multiple determination for multiple regression. The value of R^2 ranges between 0-100%. A higher value of R^2 is usually preferred as the higher the R^2 the better the model fits the data values which alternatively indicates that there is a strong relationship between the machining parameters and the response characteristics. In this experiment, linear regression analysis has been used to develop linear regression models for cutting force, surface roughness and tool wear as a function of cutting speed, feed rate and depth of cut.

Genetic Algorithm (GA)

Genetic algorithm (GA) is an evolutionary search algorithm which uses computerized search techniques based on natural selection, evolution, and natural genetics to find the optimal solution (Datta & Majumder, 2010). Specifically, GA is a population based search methodology which simulates the biological processes that allow the consecutive generations in a population to adapt to their environment (Davis, 1991) through genetic inheritance from parents to children and through survival of the fittest. Genetic Algorithm (GA) has emerged as a novel approach to

the multi-objective optimization problems due to the feature that GA does not have any mathematical requirements and can handle all types of objective functions and constraints.

Genetic Algorithm follows some fitness assignment mechanisms to determine the fitness value of individuals according to the multiple objectives. These mechanisms include vector evaluation approach, weighted sum approach, pareto based approach, compromise approach and goal programming approach. According to the perspective of methodology, Genetic Algorithm holds two basic approaches: generating approach and preference-based approach. In generating approach, GA identifies the entire set of pareto solution while preference-based approach tries to identify the preferred solution. In this study, pareto approach based on the generating approach has been used to find the optimal solution to the multi-objective optimization problem. In pareto based approach all the nondominated solutions are separated from the remaining solution and these non-dominated solutions are called Pareto solution. The preferred optimal solution is selected among the entire set of pareto optimal solutions using judgmental power of the decision maker.

The basic building block of GA is a population of individuals where each individual can be a potential solution to the problem. The individuals are provided with fitness value and they can form new individuals by undergoing stochastic transformation through two different types of genetic operations: mutation and crossover. In mutation, new individuals are created by making changes to a single individual while crossover creates new individuals with the combination of parts from two different individuals. These new individuals are called offspring. The best fit parent individuals and offspring are selected to create new population and this process continues for several generations until the algorithm converges to the best fit individuals which potentially

represent the optimal solution to the problem. The steps involved into the implementation of Multi-objective Genetic Algorithm can be shown as figure 1.

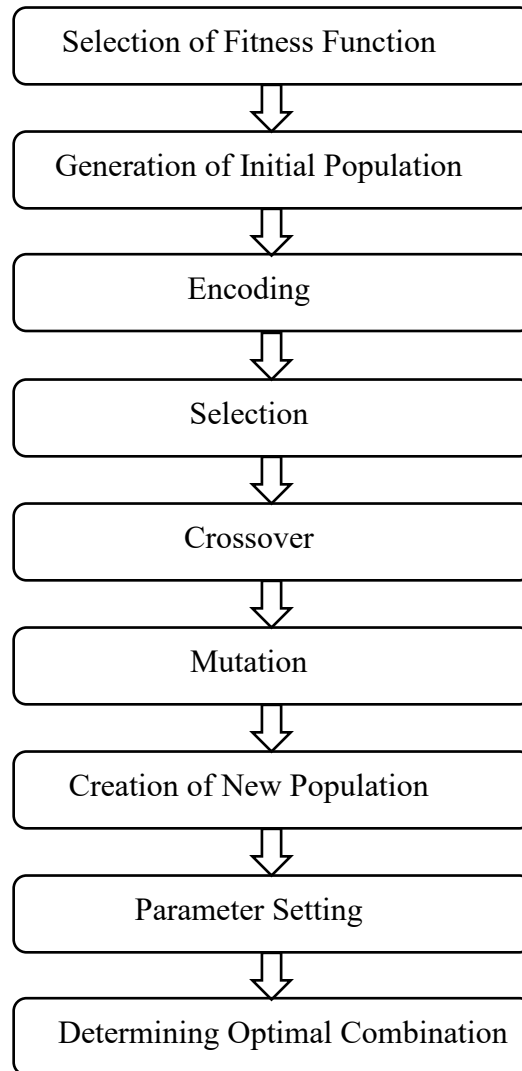


Figure 1: Multi-Objective Genetic Algorithm implementation process

Fitness function are used to measure the fitness of the individuals. In this research, three different fitness functions have been used for cutting force, surface roughness and tool wear respectively. Initial populations are generated using random functions where upper and lower bounds of decision variables are used as constraints. There are three machining parameters that

have been used in this study- cutting speed, feed rate and depth of cut. The constraints are expressed as the following equations-

$$g_1 = rand(v): v_{min} \leq v \leq v_{max} \quad (3)$$

$$g_2 = rand(f): f_{min} \leq f \leq f_{max} \quad (4)$$

$$g_3 = rand(d): d_{min} \leq d \leq d_{max} \quad (5)$$

Here, g_1 , g_2 and g_3 are constraints, v_{min} , f_{min} , and d_{min} are lower bounds, and v_{max} , f_{max} and d_{max} are upper bounds for cutting speed, feed rate and depth of cut respectively.

After generating initial population, the encoding takes place. The encoding should be performed in a proper manner because the population contains the potential solution. Best fitted populations are selected after the encoding process. In this study, tournament selection method was applied which means that two individuals were selected from the population with equal probability. After the selection is done, crossover takes place. In crossover two new off springs are created from two different parent population and then the new off springs replace two unfit individuals from the population. Mutation takes place after the crossover is finished. Crossover and mutation are considered as the basic operators of Genetic Algorithm. After mutation is completed, new populations are created, and this evolutionary process repeats until the maximum number of evolution process or generation is achieved. The Genetic algorithm usually provides a way to permanently improve the absolute fitness for everyone in the population from generation to generation and the average adaptability of the whole population. This is achieved by successive application of genetic operators of selection, crossing and mutation, thus getting better and better solutions to the problems under consideration (Cao & Wu, 1999).

Parameter setting is one of the most important steps in Genetic Algorithm. Most significant parameters are population size, maximum number of generations, mutation ratio, crossover ratio, mutation function, crossover function, lower bounds, upper bounds, and number of parameters. The efficiency of the Genetic Algorithm largely depends on the proper selection of these parameters. Smaller population size and large number of generations is required to perform the Genetic Algorithm efficiently.

After selecting the proper parameter setting, MATLAB Multi-Objective Genetic Algorithm (gamultiobj) toolbox is applied to perform the multi-objective optimization. This algorithm generates a set of nondominated pareto optimal solutions which are then plotted and the knee point on the graph is selected as the optimal solution to the corresponding multi-objective optimization problem.

Experimentation

Cutting tool and Workpiece materials

During the present study, both coated and uncoated carbide cutting tools have been used to perform turning operation on CFRP composites in CNC lathe machine. Round bars of CFRP composites have been used as workpiece. Cutting tool and workpiece have been shown in Figure 2 & 3 respectively. The cutting tool and workpiece specifications have been described in table 3.

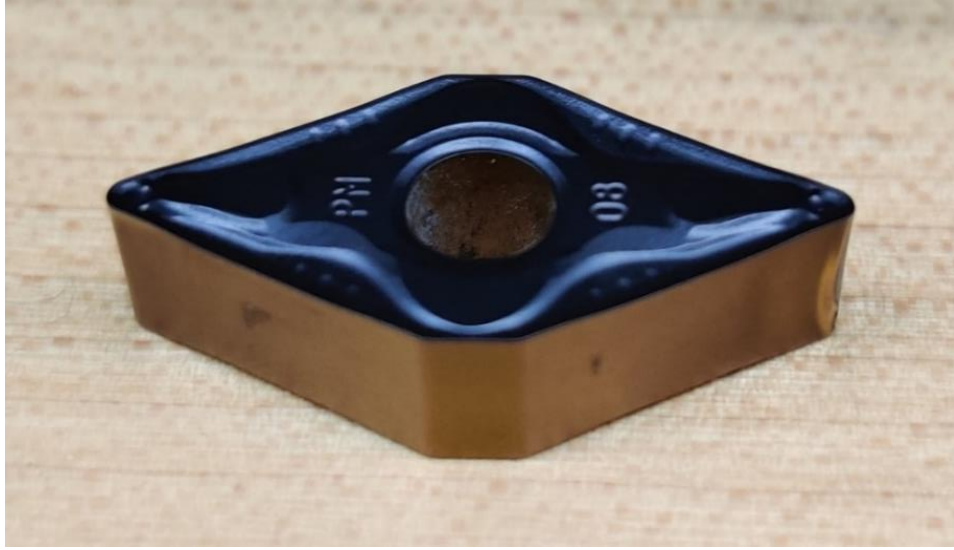


Figure 2: Cutting tool (Coated Carbide)



Figure 3: Work piece

Table 3: Cutting tool and workpiece specifications

Cutting Tool Specifications	Workpiece Specifications
Material: Carbide	Material: CFRP composite rod
Coating: Coated (TiCN/Al ₂ O ₃ /TiN) and Uncoated	Diameter: 1.5 inch
Coating Process: CVD	Fiber orientation: 0°
Corner Radius: 0.80 mm	
Included Angle: 55°	
Shape: Diamond	

Cutting Force, Tool Wear and Surface Roughness Measurement

Cutting force has been measured using Kistler 9255C Dynamometer. Signal received from the sensor is amplified by the charge amplified module. This amplified signal is sent to the DAQ (Data Acquisition) system. Then the signal is sent to the DynoWare software where the data is displayed on the monitor. Figure 4 shows the cutting force measurement set up.

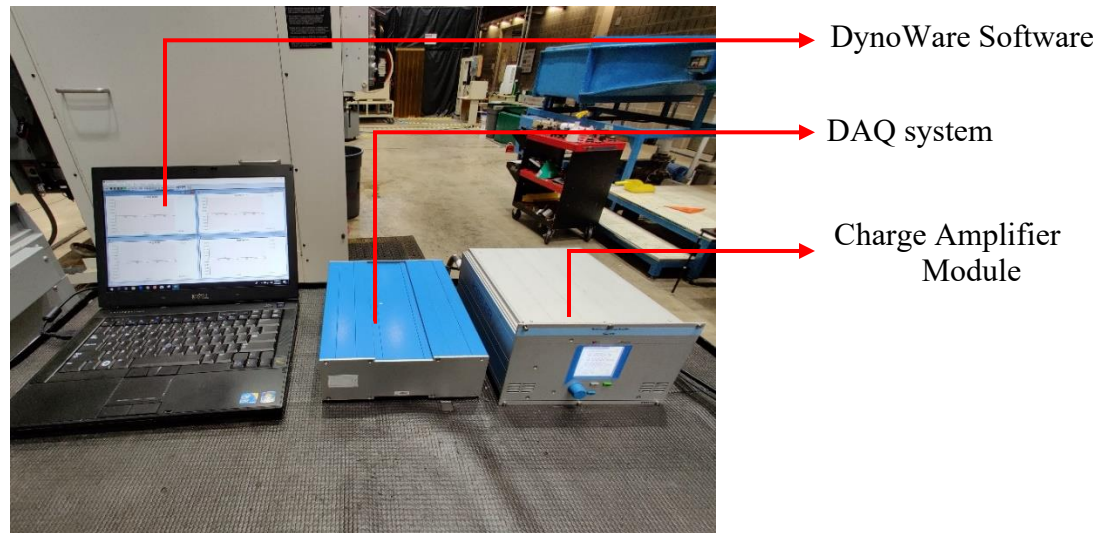


Figure 4: Cutting force measurement set up using Kistler 9255C Dynamometer

Tool wear has been measured using Keyence VHX-5000 Optical Microscope. Figure 5 illustrates the tool wear measurement set up.

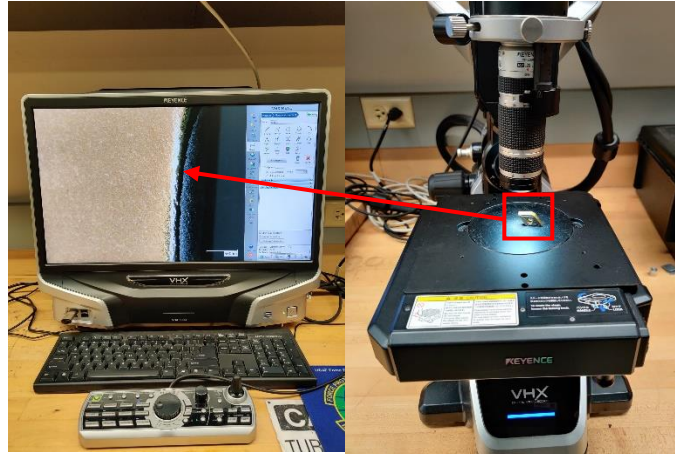


Figure 5: Tool wear measurement set up using VHX-5000 Optical Microscope

Surface roughness has been measured using MahrSurf M 300 C profilometer. This machine can measure both R_a and R_z simultaneously in a micrometer scale. Figure 6 shows the surface roughness measurement set up.



Figure 6: Surface roughness measurement set up using MahrSurf M 300 C profilometer

Experimental Setup

Machine set up mainly consists of workpiece, cutting tool and dynamometer set up.

Figure 7 illustrates a schematic diagram of experimental set up. Figure 8 shows the tool path and cutting force direction.

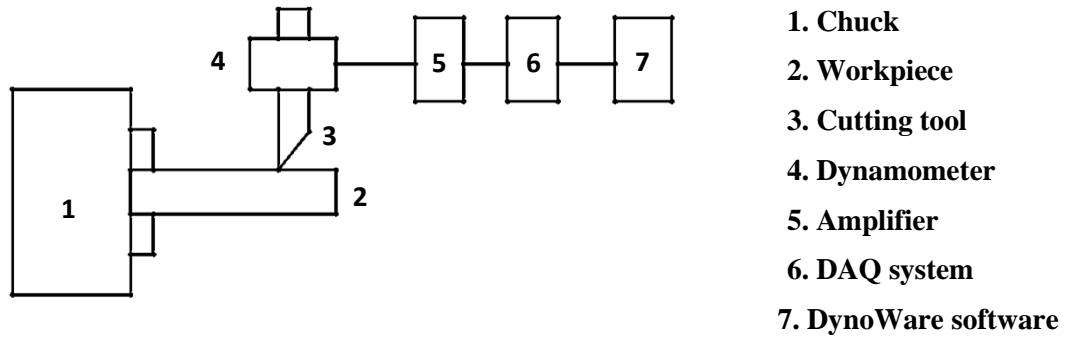


Figure 7: Schematic diagram of experimental setup

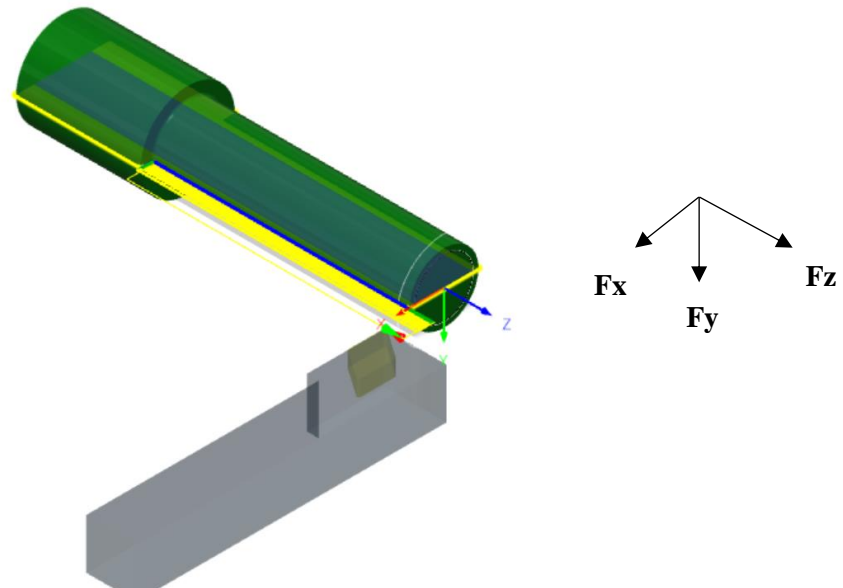


Figure 8: Tool path and cutting force direction

CHAPTER IV

RESULTS & DISCUSSION

Experimental Data

Taguchi L₉ orthogonal array was used to design the experiment and collect the data.

Table 4 and 5 represent the data collected from this experiment.

Table 4: Taguchi L₉ orthogonal array and the observed response values using coated carbide inserts

Cutting Speed (m/min)	Feed rate (mm/rev)	DOC (mm)	Cutting Force (N)	Surface Roughness (μm)	Tool Wear (mm)
75	0.05	0.1	28.38	1.14	0.33
75	0.075	0.15	34.65	1.18	0.36
75	0.1	0.2	44.73	1.21	0.40
100	0.05	0.15	27.34	1.11	0.34
100	0.075	0.2	35.42	1.17	0.38
100	0.1	0.1	43.15	1.22	0.41
125	0.05	0.2	26.31	1.12	0.35
125	0.075	0.1	31.32	1.20	0.43
125	0.1	0.15	45.64	1.25	0.44

Table 5: Taguchi L₉ orthogonal array and the observed response values using uncoated carbide inserts

Cutting Speed (m/min)	Feed rate (mm/rev)	DOC (mm)	Cutting Force (N)	Surface Roughness (μm)	Tool Wear (mm)
75	0.05	0.1	27.5	1.22	0.40
75	0.075	0.15	35.53	1.31	0.42
75	0.1	0.2	43.85	1.42	0.44
100	0.05	0.15	26.22	1.15	0.41
100	0.075	0.2	34.54	1.29	0.45
100	0.1	0.1	44.04	1.40	0.48
125	0.05	0.2	26.43	1.14	0.47
125	0.075	0.1	31.2	1.37	0.50
125	0.1	0.15	44.77	1.46	0.53

Taguchi Analysis: Effects of Machining Parameters on Turning Performance

Characteristics

The effects of machining parameters on turning performance characteristics are analyzed using response tables of cutting parameters which are constructed using the mean values of cutting parameters at a particular level. The optimal level of cutting parameters is selected by analyzing the main effect plot of S/N ratios of cutting parameters.

Coated Carbide

Effects of Machining Parameters on Cutting Force Table 6 represents the response table of the means of cutting forces. It was observed that the machining parameter that influences the cutting forces most is the feed rate (Rank 1) followed by the Dept of cut (DoC) (Rank 2) and cutting speed (Rank 3). Similar result was found in the literature where the researchers reported that feed rate is the most influencing factor for cutting force during turning of CFRP composites (Rajasekaran, Gaitonde, et al., 2013). Figure 9 illustrates the effects of machining parameters on cutting force. It was observed that cutting force decreases with the increase of cutting speed. Higher cutting speed lowers the material removal rate due to the decreased contact area between workpiece and cutting tool which ultimately results in a lower cutting force. It was observed that cutting force increases with the increase of feed rate. This is because the higher feed rate increases the contact area between workpiece the cutting tool leading to a higher material removal rate which results in an increase of cutting force. From figure 9, it was also observed that cutting force increases with the increase of depth of cut (DoC) and after coming to a maximum value it starts to decrease with the increase of feed rate. Higher depth of cut results in a higher material removal rate and increased friction between cutting tool and workpiece. As a result, the cutting force increases.

Table 6: Response table for means of Cutting force (Coated Carbides)

Level	Means of Cutting Force (N) for corresponding parameter level		
	Cutting Speed	Feed	DoC
1	35.92	27.34	34.28
2	35.30	33.80	35.88
3	34.42	44.51	35.49
Delta (max-min)	1.50	17.16	1.59
Rank	3	1	2

Contour plots were used to explain the relation between response characteristic and two different machining parameters. Figure 10 describes the relation of cutting force with cutting speed and feed rate. It was observed that higher cutting speed with lower feed rate generates lower cutting force. As long as the feed rate is lower, the cutting force will be lower irrespective of cutting speed which can be seen in the lower and upper left corners of figure 10. Cutting speed around 120 m/min with feed rate around 0.05 mm/rev can provide a lower cutting force around 26 N. Figure 11 shows that higher cutting speed with lower depth of cut can provide lower cutting force. It was found that cutting speed around 100 m/min and depth of cut around 0.15 mm generates cutting force around 27 N. From figure 12 it can be observed that lower feed rates always generate lower cutting force irrespective of depth of cut. We could see that feed rate below 0.05 mm/rev is capable to generate the lower level of force around 28 N with the variation of depth of cut between 0.1-0.2 mm.

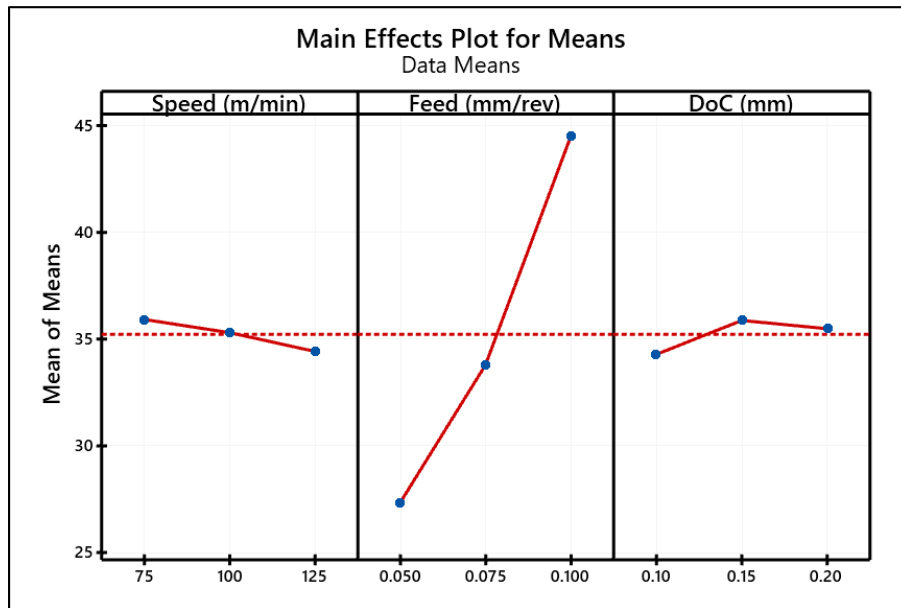


Figure 9: Effects of machining parameters on cutting force (Coated Carbides)

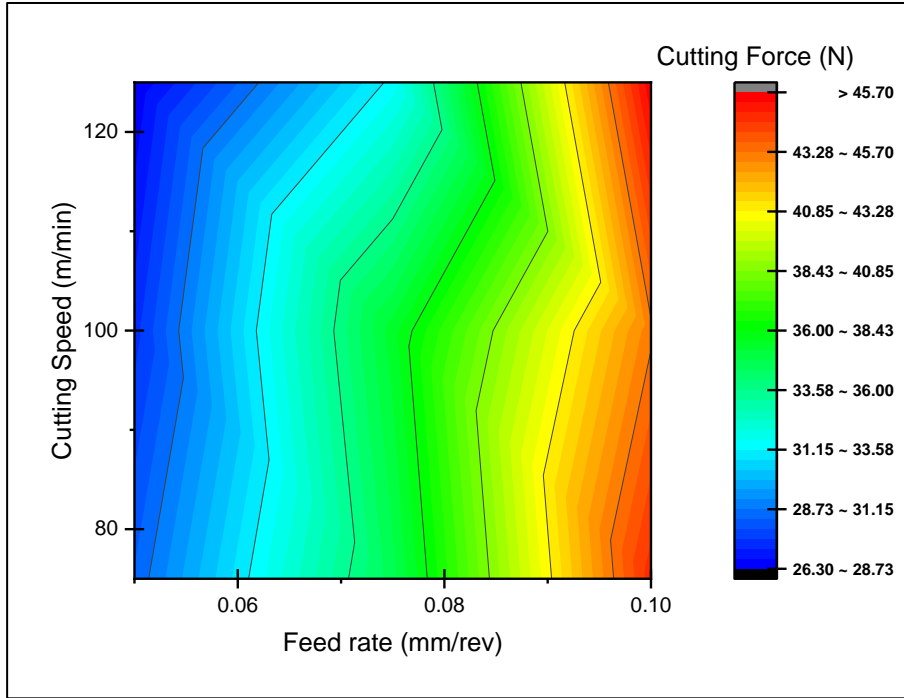


Figure 10: Contour plot for cutting force: cutting speed vs feed rate (Coated Carbides)

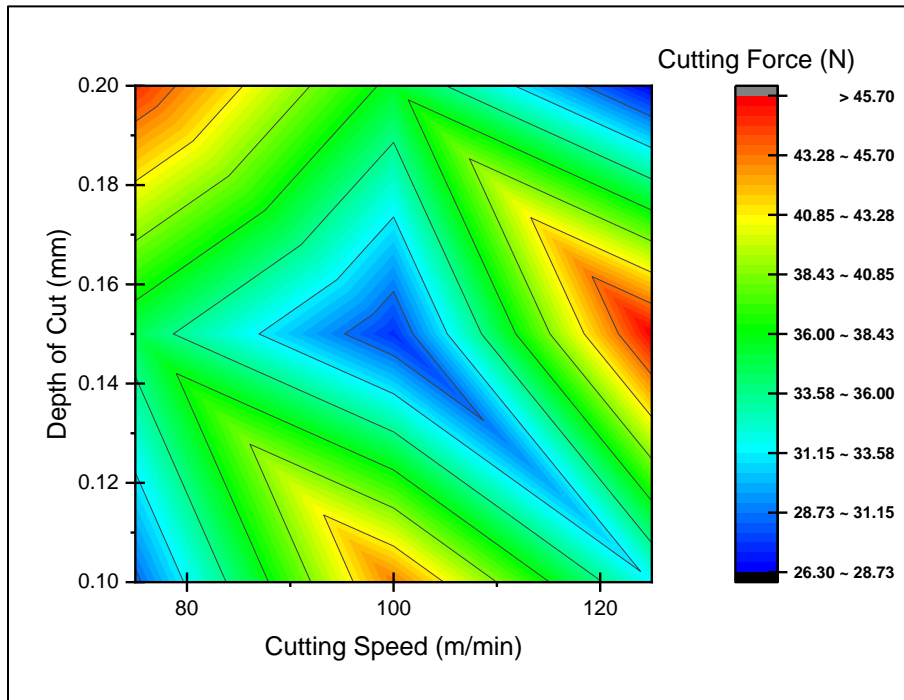


Figure 11: Contour plot for cutting force: cutting speed vs depth of cut (Coated Carbides)

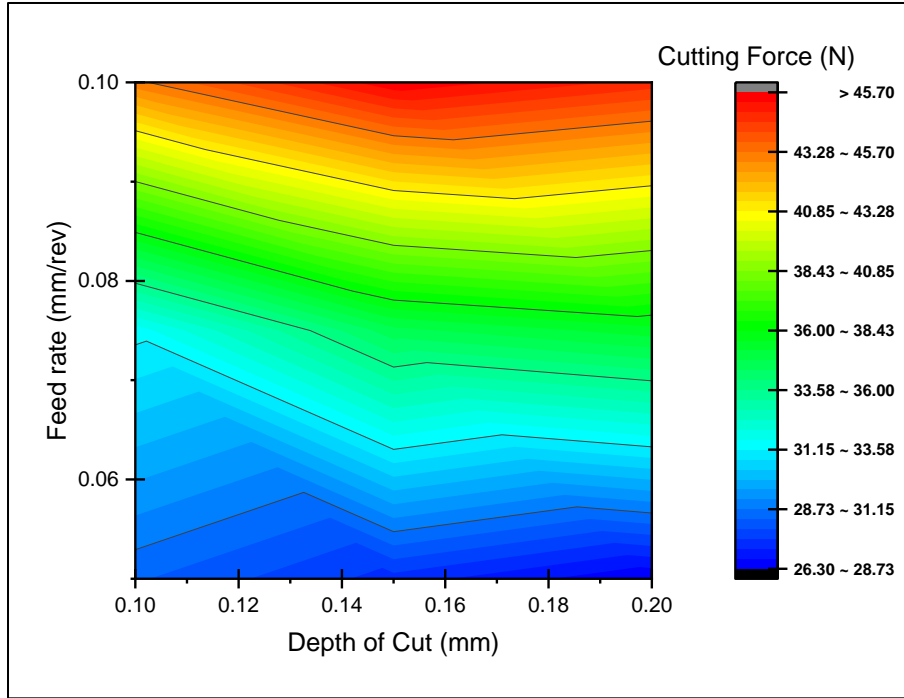


Figure 12: Contour plot for cutting force: feed rate vs depth of cut (Coated Carbides)

Response table for S/N ratios of cutting force has been shown in table 7. Main effect plot for S/N ratios obtained for cutting force has been shown in figure 13. Higher S/N ratio represents the least variation between expected value and measured value of an output characteristic. From figure 13, it was observed that the highest S/N ratio obtained for cutting force are cutting speed at 125 m/min, feed rate at 0.05 mm/rev and depth of cut at 0.1 mm, respectively. So, the optimal machining parameters to obtain low cutting force were predicted by Taguchi method as $v = 125 \text{ m/min}$, $f = 0.05 \text{ mm/rev}$, and $d = 0.1 \text{ mm}$ which can be represented as $v_3 - f_1 - d_1$. The corresponding level values for the parameters were bolded in table 7.

Table 7: Response table for signal to noise (S/N) ratios of Cutting force (Coated Carbides)

Symbol	Machining Parameters	S/N ratio			Max-Min	Rank
		Level 1	Level 2	Level 3		
v	Cutting speed (m/min)	-30.96	-30.81	-30.50	0.45	2
f	Feed rate (mm/rev)	-28.73	-30.57	-32.97	4.23	1
d	Depth of Cut (mm)	-30.56	-30.91	-30.80	0.35	3

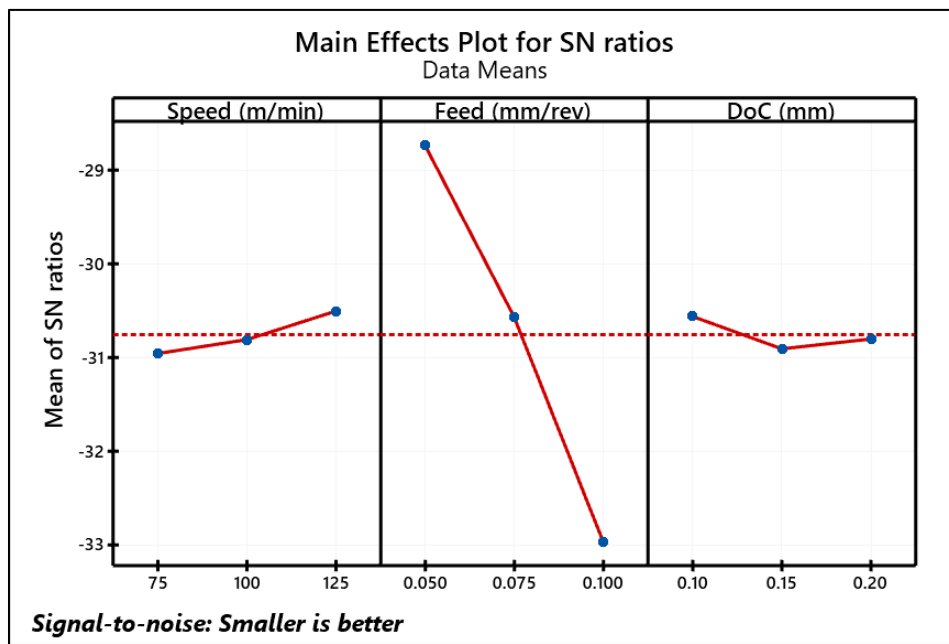


Figure 13: Main effect plot of S/N ratios for cutting force (Coated Carbides)

Effects of Machining Parameters on Surface Roughness Table 8 represents the response table of means for surface roughness. It was observed that the machining parameter that influences the surface roughness most is the feed rate (Rank 1) followed by cutting speed (Rank 2) and Depth of cut (Rank 3). Similar result has been found in the literature (Rajasekaran et al., 2012b). Figure 14 describes the effects of machining parameters on surface roughness. It was

observed that surface roughness decreases with the increases of cutting speed initially and then tends to increase again with the increase of cutting speed. This is because higher cutting speed reduces the contact length between chip and tool which leads to reduced friction in the machining surface. As a result, the fiber fracture and the fiber pulling out get decreased, hence the surface roughness decreases. However, the increase of cutting speed beyond the optimal point increases the machine tool vibration which increases the surface roughness eventually.

Table 8: Response table for means of Surface roughness (Coated Carbides)

Level	Means of Surface Roughness (μm) for corresponding parameter level		
	Cutting Speed	Feed rate	Depth of Cut
1	1.180	1.126	1.188
2	1.168	1.186	1.181
3	1.192	1.228	1.171
Delta	0.024	0.101	0.017
Rank	2	1	3

It was observed that the surface roughness increases with the increase of feed rate. Higher feed rate increases the contact area between workpiece and cutting tool which results in increased feed force. The increased feed force increases the fiber fracture and fiber pullout on the outside surface of the workpiece materials leading to an increase of surface roughness. Similar outputs have been found in the literature (Rajasekaran et al., 2012b). It was observed that the surface roughness decreases with the increase of depth of cut. This is due to the fact that the increased depth of cut reduces the friction between cutting tool and chips which reduces the fiber pullout and fiber fracture leading to a decreased of surface roughness. Figure 15 shows the optical microscopic view of machined surface obtained at cutting speed of 100 m/min, feed rate of 0.05 mm/rev and depth of cut 0.15 mm.

Figure 16-18 shows the relation of surface roughness with cutting speed, feed rate and depth of cut. It was observed that lower feed rate with higher cutting speed leads to lower surface roughness. This result coincides with the previous research (Rajasekaran et al., 2012b). Cutting speed around 100 m/min and feed rate around 0.05 mm/rev results in a lower surface roughness value around 1.12 μm . Higher cutting speed and higher depth of cut generates lower surface roughness. Cutting speed around 100 m/min with the depth of cut around 0.15 mm can provide the lower surface roughness around 1.11 μm . It was observed that lower feed rate and higher depth of cut also provides lower surface roughness. Feed rate close to 0.05 mm/rev with depth of cut around 0.15 mm generates the lower surface roughness around 1.13 μm .

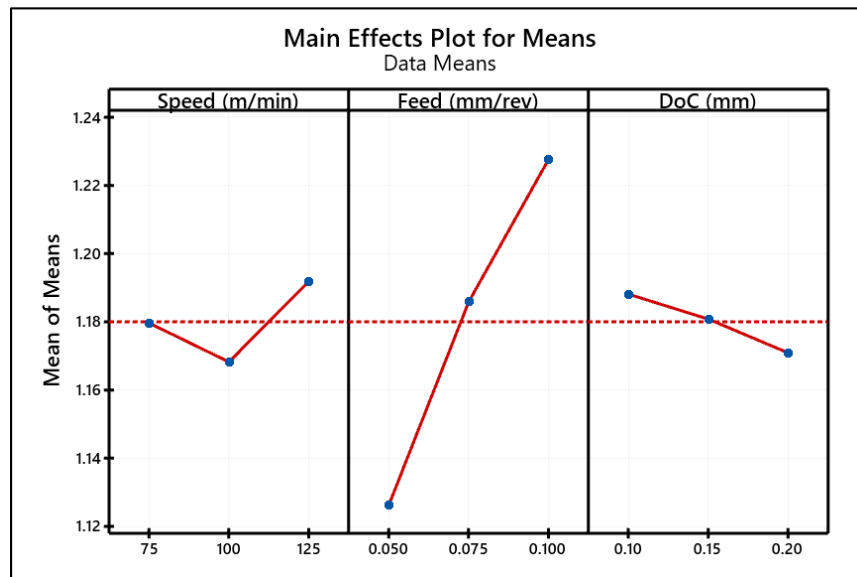


Figure 14: Effects of machining parameters on surface roughness (Coated Carbides)



Figure 15: Optical microscopic view of machined surface obtained at cutting speed of 100 m/min, feed rate of 0.05 mm/rev and depth of cut 0.15 mm

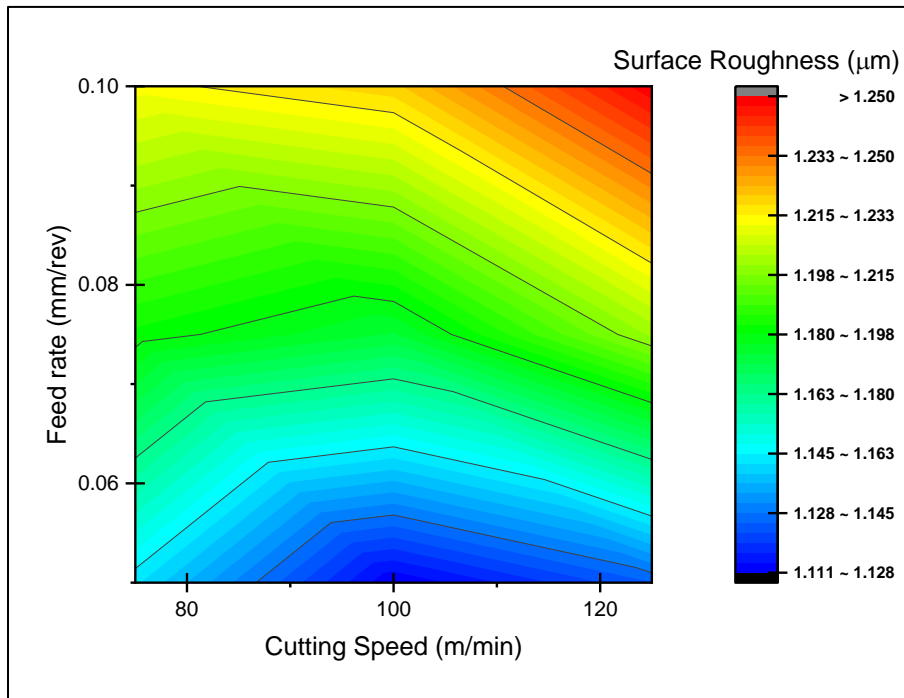


Figure 16: Contour plot for surface roughness: cutting speed vs feed rate (Coated Carbides)

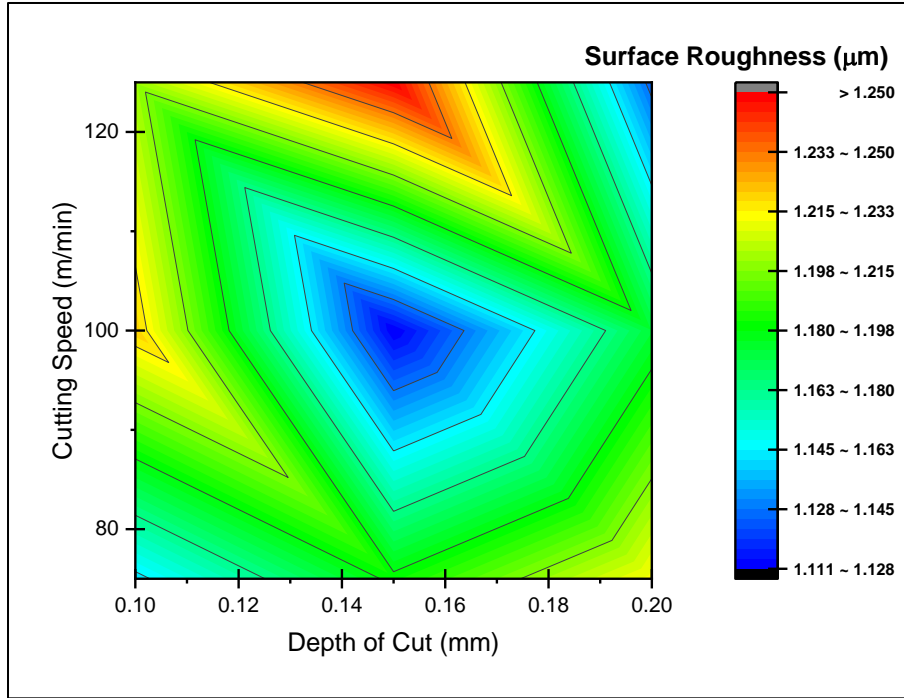


Figure 17: Contour plot for surface roughness: Cutting speed vs depth of cut (Coated Carbides)

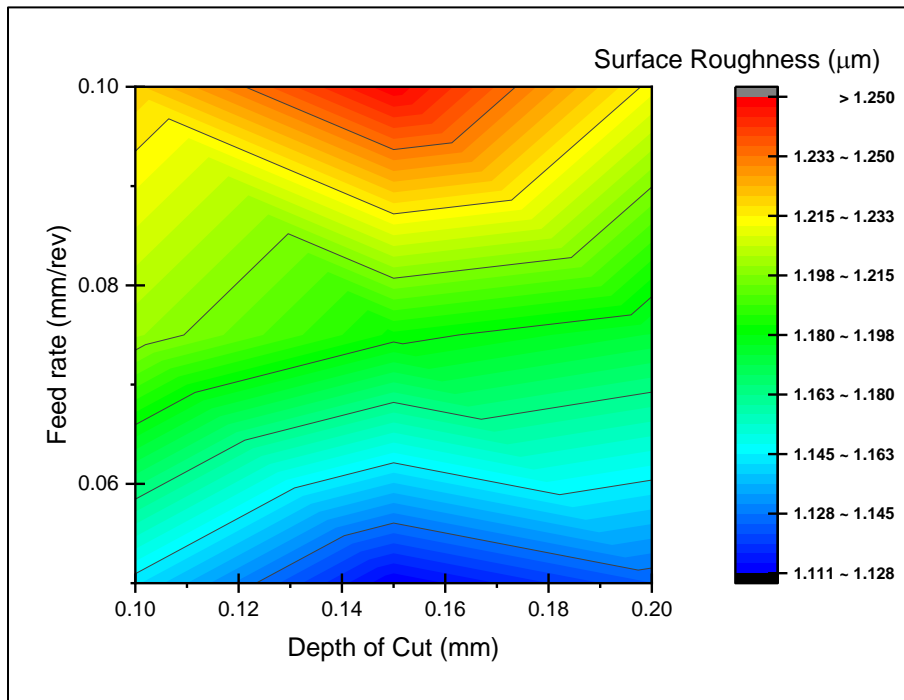


Figure 18: Contour plot for surface roughness: Feed rate vs depth of cut (Coated Carbides)

Response table for S/N ratios of surface roughness has been shown in table 9. Main effect plot for S/N ratios obtained for surface roughness has been shown in figure 19. It was observed that the highest S/N ratio obtained for surface roughness are cutting speed at 100 m/min, feed rate at 0.05 mm/rev and depth of cut at 0.2 mm. So, the optimal machining parameters for obtaining lower surface roughness were predicted by the Taguchi analysis as $v = 100 \text{ m/min}, f = 0.05 \text{ mm/rev}$, and $d = 0.2 \text{ mm}$ which was represented as $v_2 - f_1 - d_3$. The corresponding level values for parameters were bolded in table 9.

Table 9: Response table for signal to noise (S/N) ratios of Surface roughness (Coated Carbides)

Symbol	Machining Parameters	S/N ratio			Max-Min	Rank
		Level 1	Level 2	Level 3		
v	Cutting speed (m/min)	-1.433	-1.344	-1.517	0.173	2
f	Feed rate (mm/rev)	-1.032	-1.481	-1.781	0.749	1
d	Depth of Cut (mm)	-1.494	-1.434	-1.366	0.128	3

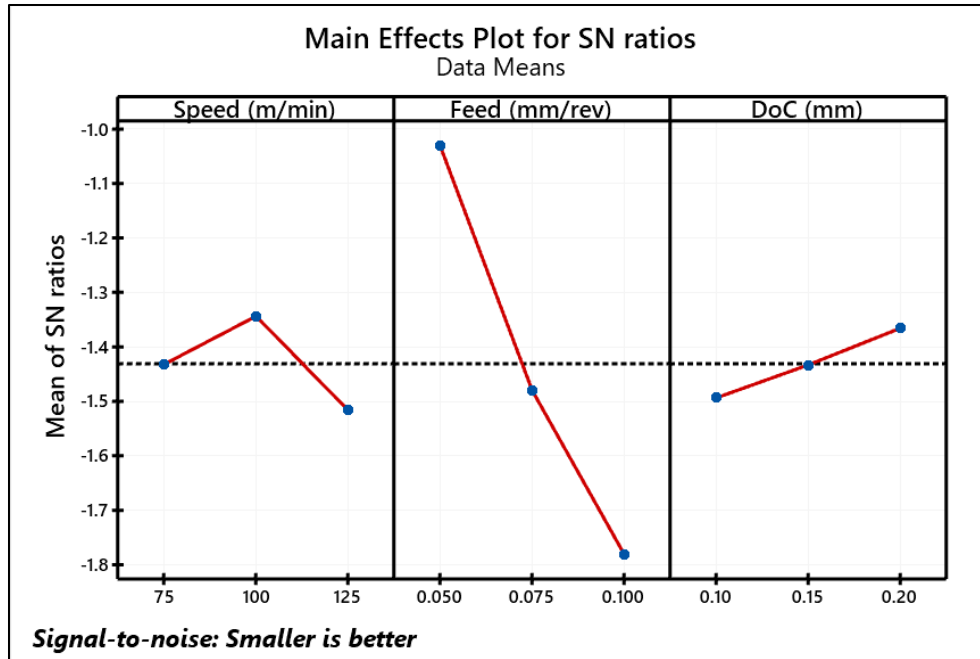


Figure 19: Main effect plots for S/N ratios of surface roughness (Coated Carbides)

Effects of machining parameters on Tool wear Table 10 shows the response table for means of tool wear. It was observed that the machining parameter that influenced the tool wear most is the feed rate (Rank 1) followed by the cutting speed (Rank 2) and depth of cut (Rank 3). Figure 20 represents the effects of machining parameters on tool wear. It was observed that tool wear increases with the increase of cutting speed and feed rate. Higher cutting speed and feed rate increases the friction in machining surface and vibration of the workpiece material leading to an increase of tool wear. It was observed that tool wear decreases with the increase of depth of cut. This may be due to the fact that turning operation of CFRP usually produces powder like chips and the higher depth of cut reduces the friction between the chips and cutting tool which leads to a decrease of tool wear.

Table 10: Response table for means of tool wear (coated carbides)

Level	Mean of Tool Wear (mm) for corresponding parameter level		
	Cutting Speed	Feed	DoC
1	0.3647	0.3407	0.3903
2	0.3770	0.3900	0.3817
3	0.4070	0.4180	0.3767
Delta	0.0423	0.0773	0.0137
Rank	2	1	3

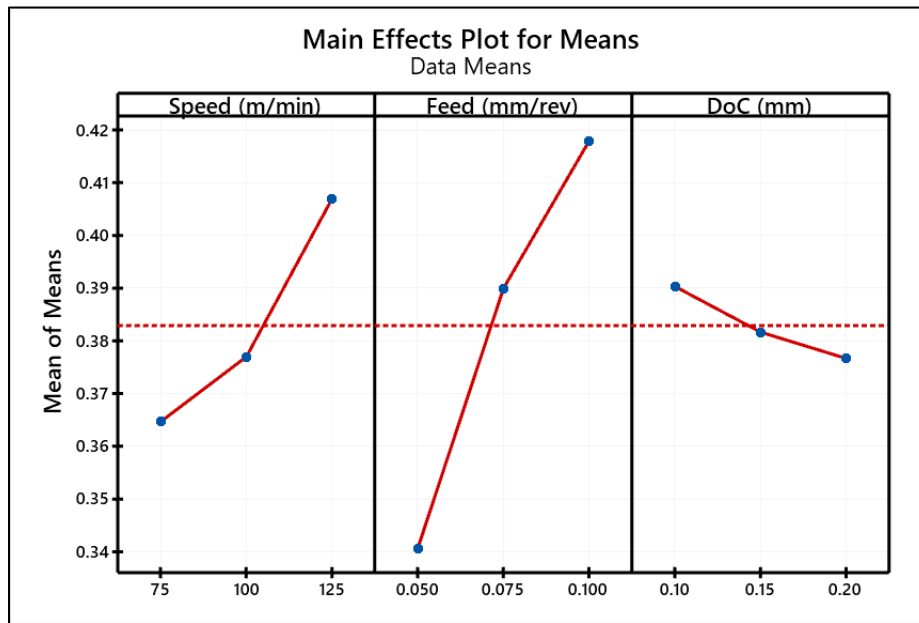


Figure 20: Effect of machining parameters on tool wear (Coated Carbides)

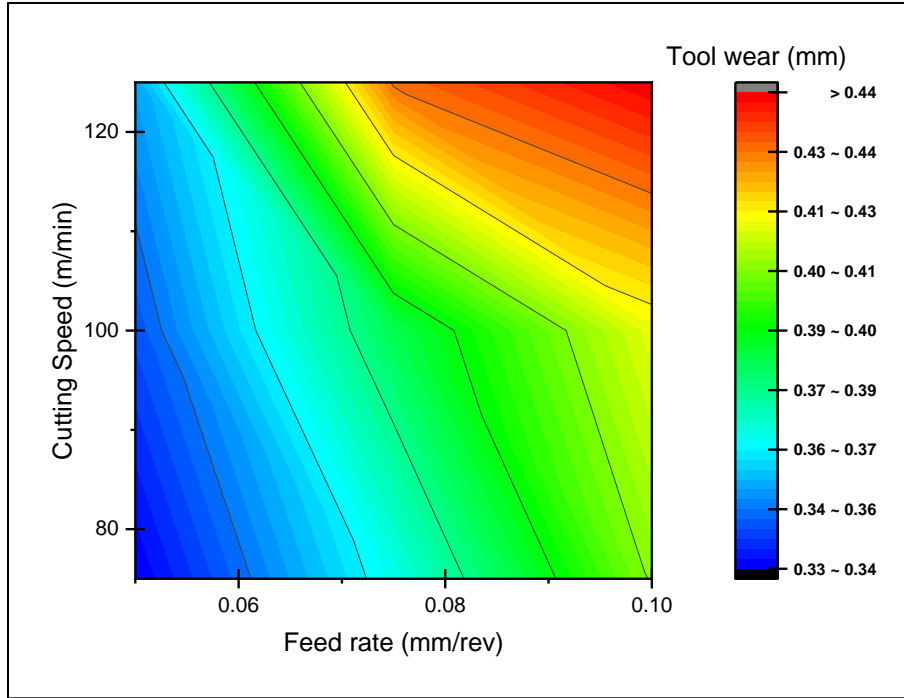


Figure 21: Contour plot for tool wear: cutting speed vs feed rate (Coated Carbides)

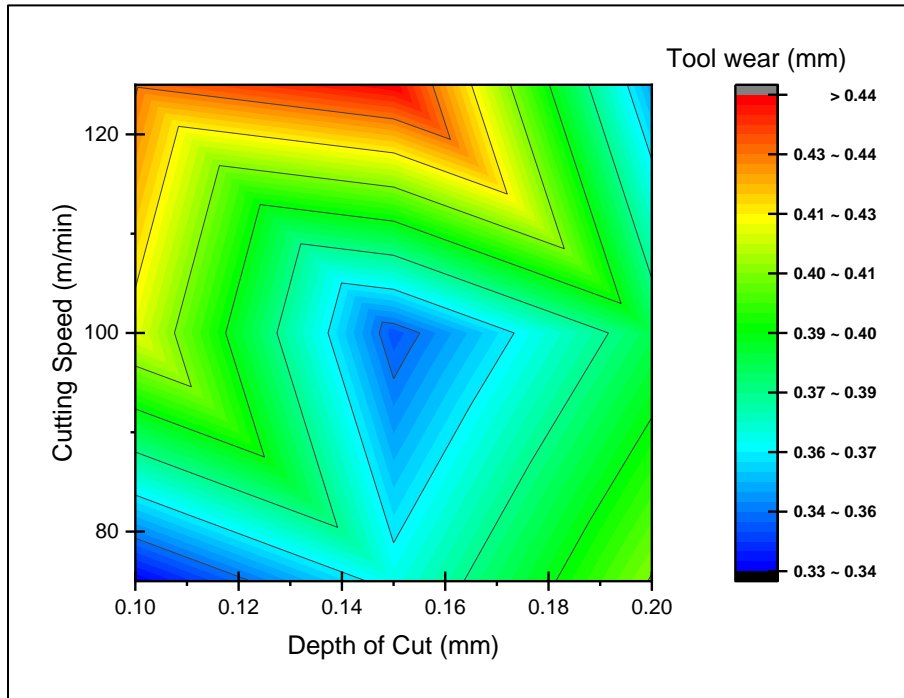


Figure 22: Contour plot for tool wear: cutting speed vs depth of cut (Coated Carbides)

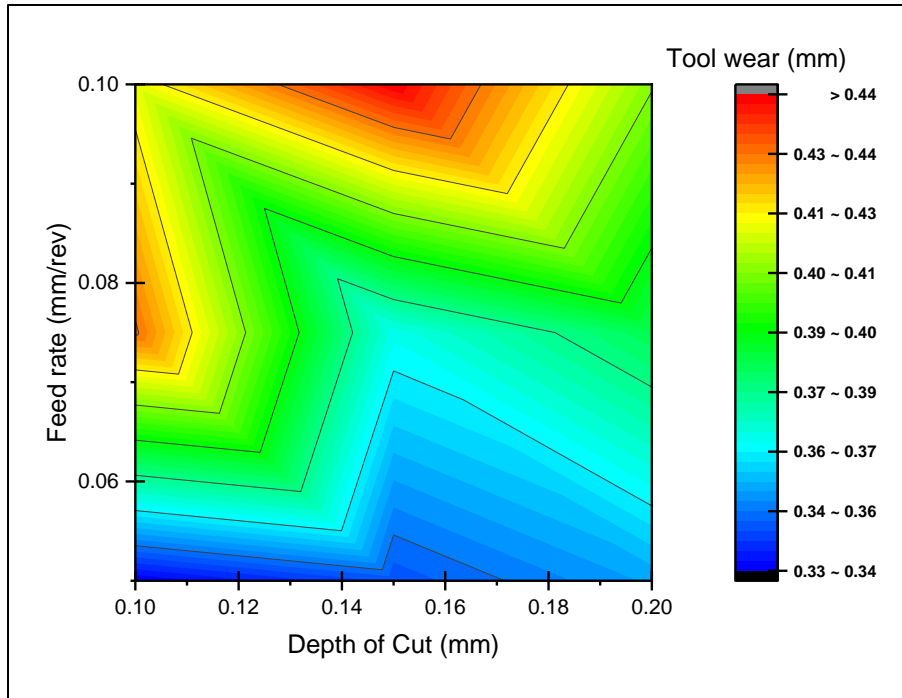


Figure 23: Contour plot for tool wear: feed rate vs depth of cut (Coated Carbides)

Figure 21 shows the relation of tool wear with cutting speed and feed rate. It was observed that lower cutting speed with lower feed rate results in lower tool wear. The lower left corner of the graph shows the lowest tool wear which corresponds to the cutting speed near 80 m/min with feed rate around 0.05 mm/rev and the lower tool wear close to 0.33 mm. Figure 22 describes that lower tool wear can be obtained at lower cutting speed and lower depth of cut. Cutting speed close to 70 m/min along with depth cut near 0.1 mm can provide the lower tool wear close to 0.33 mm. Moreover, cutting speed around 95 m/min along with depth of cut around 0.15 mm can also generate a lower value of tool wear near 0.36 mm. Figure 23 shows that lower feed rate with lower depth of cut lead to a generation of lower tool wear. It was observed that feed rate near 0.05 mm/rev and depth of cut between 0.1 mm-0.16 mm can generate a lower level of tool wear close to 0.33-0.36 mm.

Response table for S/N ratios of tool wear has been shown in table 11. Main effect plot for S/N ratios obtained for surface roughness has been shown in figure 24. It was observed that the highest S/N ratio obtained for tool wear are cutting speed at 75 m/min, feed rate at 0.05 mm/rev and depth of cut at 0.2 mm. So, the optimal machining parameters to obtain lower tool wear were predicted by Taguchi method as $v = 75 \text{ m/min}$, $f = 0.05 \text{ mm/rev}$, and $d = 0.2 \text{ mm}$ which are represented as $v_1 - f_1 - d_3$. The corresponding level values for the parameters are bolded in table 11.

Table 11: Response table for signal to noise (S/N) ratios of tool wear (Coated Carbides)

Symbol	Machining Parameters	S/N ratio			Max-Min	Rank
		Level 1	Level 2	Level 3		
v	Cutting speed (m/min)	8.789	8.498	7.854	0.935	2
f	Feed rate (mm/rev)	9.356	8.201	7.584	1.772	1
d	Depth of Cut (mm)	8.226	8.421	8.494	0.269	3

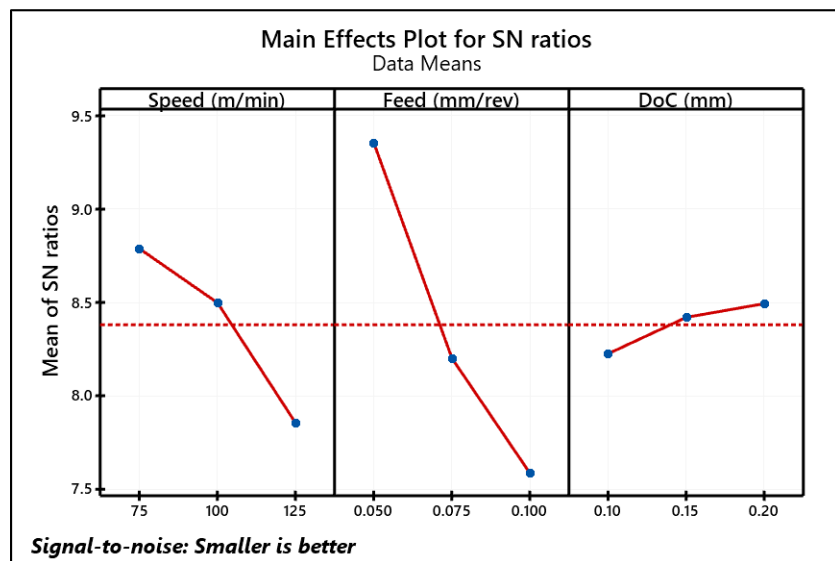


Figure 24: Main effect plots for S/N ratios of tool wear (Coated Carbides)

Uncoated Carbide

Effects of Machining parameters on Cutting force Table 12 represents the response table for means of cutting force. It was observed that the machining parameter that influences the cutting force most was the feed rate (Rank 1) followed by depth of cut (Rank 2) and cutting speed (Rank 3). Previous researchers also found that feed rate is the most influencing factor for cutting force during turning of CFRP composites (Rajasekaran, Gaitonde, et al., 2013). Figure 25 illustrates the effects of machining parameters on cutting force. It was observed that cutting force decreases with the increase of cutting speed. With the increase of cutting speed the contact area between workpiece and cutting tool decreases which reduces the material removal rate leading to a decrease of cutting force. It was observed that the cutting force increases with the increase of feed rate and depth of cut. With the increase of feed rate and depth of cut the material removal rate increase due to increased contact area between workpiece and tool material. Moreover, the friction on the machining interface gets increased. As a result, the cutting force increases.

Table 12: Response table for means of Cutting force (Uncoated Carbides)

Level	Means of Cutting Force (N) for corresponding parameter level		
	Cutting Speed	Feed	DoC
1	35.63	27.05	34.58
2	35.60	34.09	36.17
3	34.13	44.22	34.61
Delta	1.49	17.17	1.59
Rank	3	1	2

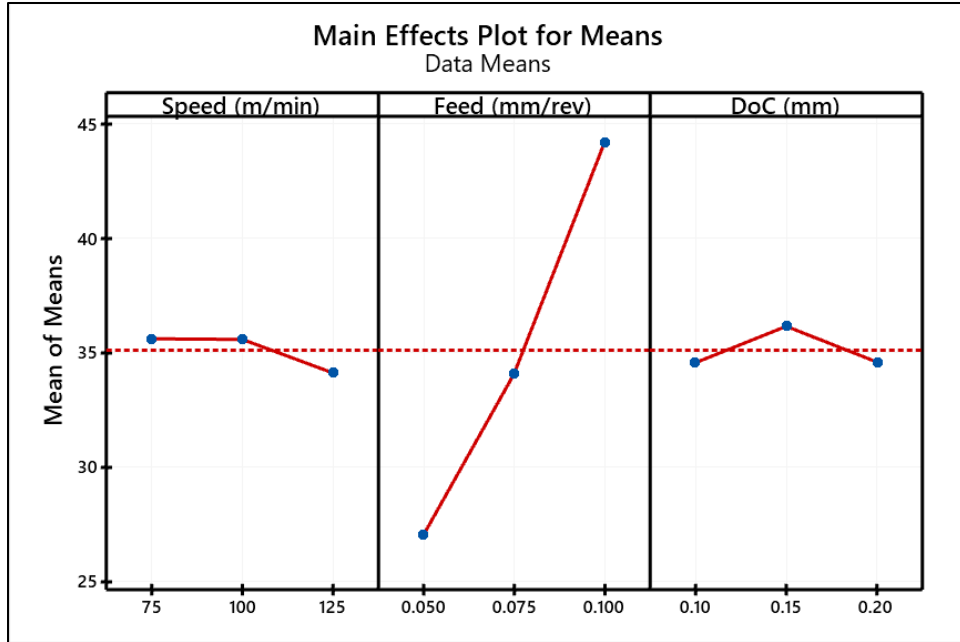


Figure 25: Effects of machining parameters on cutting force (Uncoated Carbides)

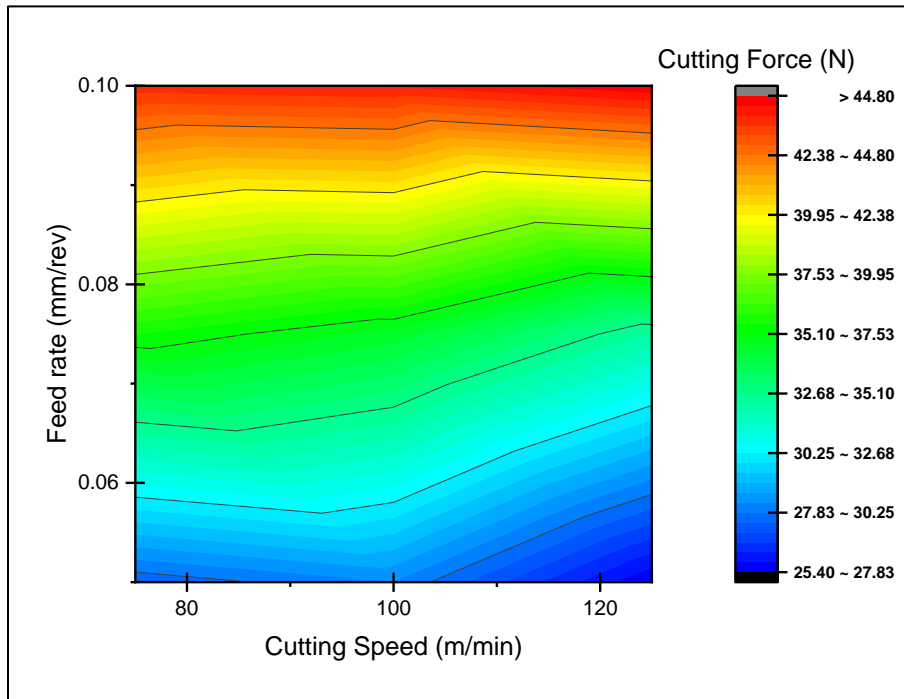


Figure 26: Contour plot for cutting force: cutting speed vs feed rate (Uncoated Carbides)

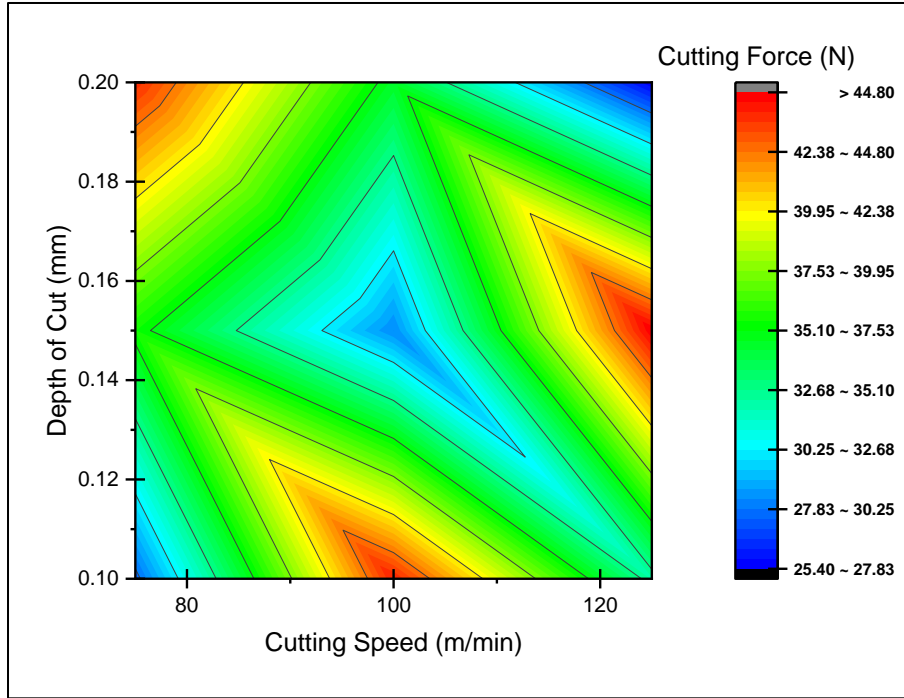


Figure 27: Contour plot for cutting force: cutting speed vs depth of cut (Uncoated Carbides)

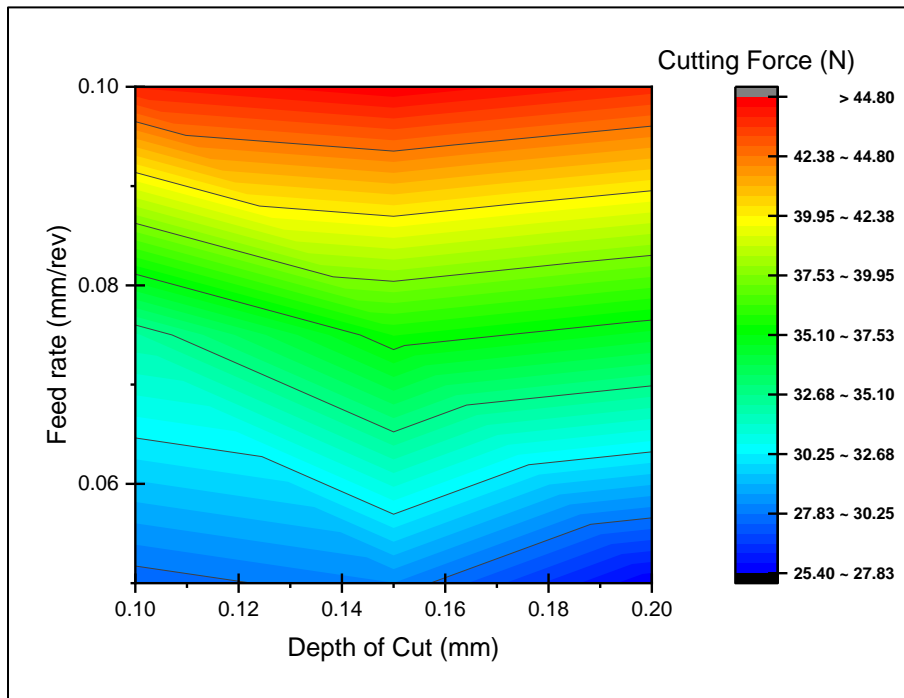


Figure 28: Contour plot for cutting force: feed rate vs depth of cut (Uncoated Carbides)

Figure 26 shows the relation of cutting force with cutting speed and feed rate. It was found that higher cutting speed with lower feed rate leads to a lower cutting force. The lower right corner of the graph shows the lowest cutting force which represents the cutting speed around 120 m/min and the feed rate close to 0.05 mm/rev with a cutting force near 26 N. From figure 27, it can be found that higher cutting speed with lower depth of cut can provide a lower cutting force, but it is very difficult to find a significant relation of cutting force with cutting speed as it has the least effect on cutting force as indicated in table 10 (rank 3). Cutting speed around 100 m/min with the depth of cut near 0.15 mm can generate lower values of cutting force around 30 N. Figure 28 shows that lower cutting force can also be obtained using lower levels of feed rate and depth of cut. It was observed that feed rate close to 0.05 mm/rev can generate lower cutting force near 27 N when the depth of cut between 0.1-0.2 mm is maintained.

Response table for signal to noise (S/N) ratio of cutting force has been shown in table 13. Main effects plot of S/N ratios for cutting force has been shown in figure 29. It was observed that the highest S/N ratios obtained for cutting force are cutting speed at 125 m/min, feed rate at 0.05 mm/rev and depth of cut at 0.1 mm. So, the optimal machining parameters to obtain lower cutting force were $v = 125 \text{ m/min}$, $feed \text{ rate} = 0.05 \text{ mm/rev}$, and $d = 0.1 \text{ mm}$ which are represented as $v_3 - f_1 - d_1$. Corresponding level values of the parameters are bolded in table 13.

Table 13: Response table for signal to noise (S/N) ratio of cutting force (Uncoated Carbides)

Symbol	Machining Parameters	S/N ratio			Max-Min	Rank
		Level 1	Level 2	Level 3		
v	Cutting speed (m/min)	-30.88	-30.88	-30.43	0.46	2
f	Feed rate (mm/rev)	-28.63	-30.65	-32.91	4.28	1
d	Depth of Cut (mm)	-30.61	-31.01	-30.57	0.44	3

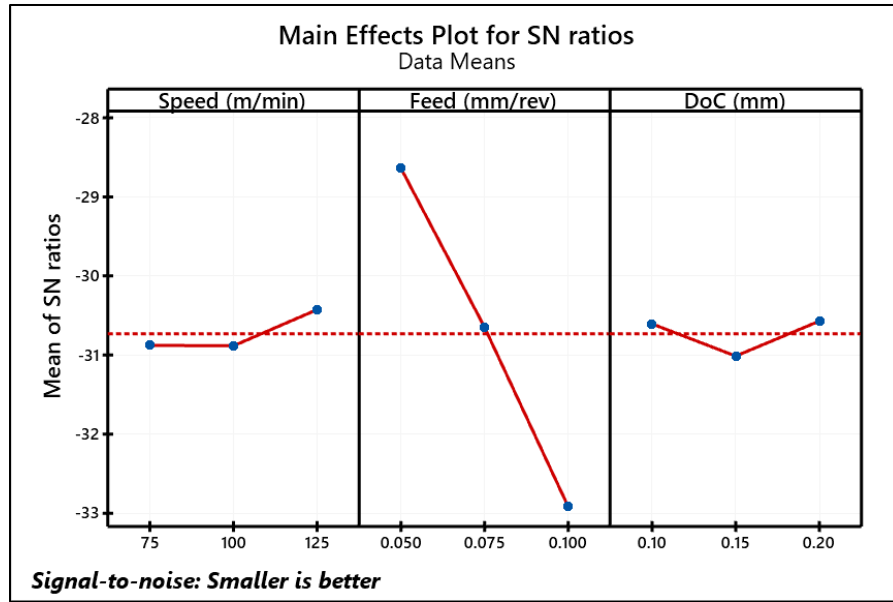


Figure 29: Main effects plot for S/N ratio of cutting force (Uncoated Carbides)

Effects of Machining Parameters on Surface Roughness Response table for means of surface roughness has been shown in table 14. It was found that the machining parameter that influences the surface roughness most is the feed rate (Rank 1) followed by depth of cut (Rank 2) and cutting speed (Rank 3). Figure 30 illustrates the effects of machining parameters on surface roughness. It was observed that surface roughness decreases with the increases of cutting speed initially and then tends to increase again with the increase of cutting speed. This is because higher cutting speed reduces the contact length between chip and tool which leads to reduced friction in the machining surface. As a result, the fiber fracture and the fiber pulling out get decreased, hence the surface roughness decreases. However, the increase of cutting speed beyond the optimal point increases the machine tool and workpiece vibration which increases the surface roughness eventually.

Table 14: Response table of means of surface roughness (Uncoated Carbides)

Level	Means of Surface Roughness (μm) for corresponding parameter level		
	Cutting Speed	Feed	DoC
1	1.317	1.172	1.334
2	1.282	1.325	1.310
3	1.325	1.427	1.281
Delta	0.044	0.255	0.053
Rank	3	1	2

From figure 30, it was observed that the surface roughness increases with the increase of feed rate. This is due to the fact that higher feed rate increases the contact area between workpiece and cutting tool which increases the material removal rate. Higher material removal rate increases the feed force. The increased feed force increases the fiber fracture and fiber pullout on the outside surface of the workpiece materials leading to an increase of surface roughness. It was observed that surface roughness decreases with the increase of depth of cut. While turning the CFRP rod, powder like chips is generated. Due to the high temperature at the cutting zone, these chips get attached to the surface of workpiece. Higher depth of cut reduces the friction between these chips and cutting tool which leads to a decrease in surface roughness. Figure 31 shows the powder like chips produced during turning of CFRP composites in this experiment.

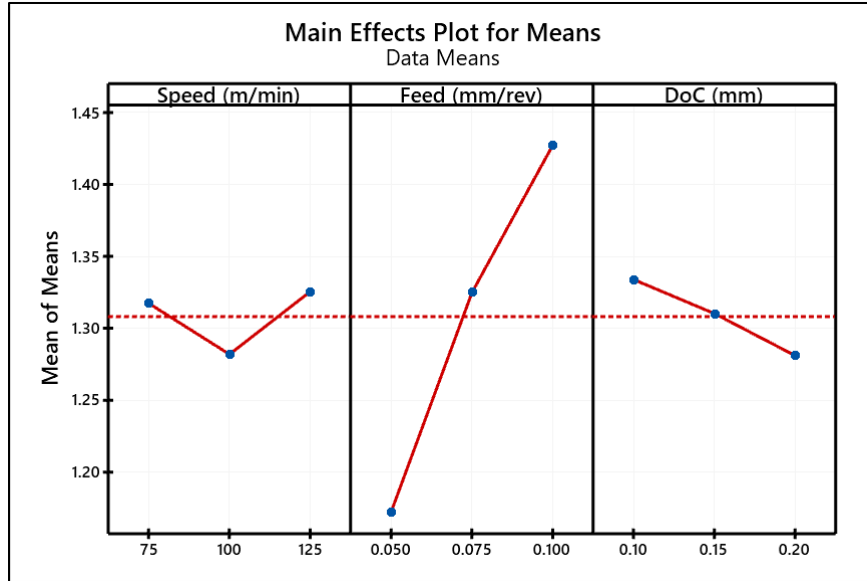


Figure 30: Effects of machining parameters on surface roughness (Uncoated Carbides)



Figure 31: Powder like chips produced during turning process of CFRP

Contour plot in figure 32 explains the relation of surface roughness with cutting speed and feed rate. It was observed that lower level of feed rate with higher level of cutting speed generates lower surface roughness. Feed rate around 0.05 mm/rev with the cutting speed above 100 m/min can provide a lower level of surface roughness near 1.14-1.18 μm . Figure 33 describes that higher cutting speed and higher depth of cut results in lower surface roughness. Cutting speed around 100 m/min with the depth of cut near 0.15 mm leads to a lower surface roughness value around 1.16 μm . Figure 34 illustrates that lower feed rate and higher depth of cut results in lower surface roughness. Depth of cut above 0.14 mm with feed rate near 0.05 mm/rev can generate lower surface roughness which is close to 1.15 μm .

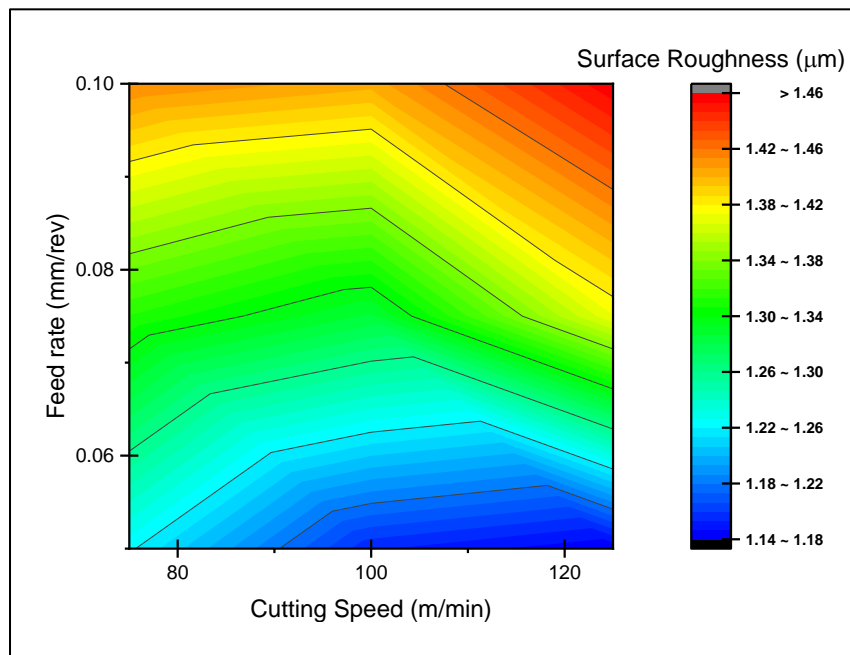


Figure 32: Contour plot for surface roughness: Cutting speed vs feed rate (Uncoated Carbides)

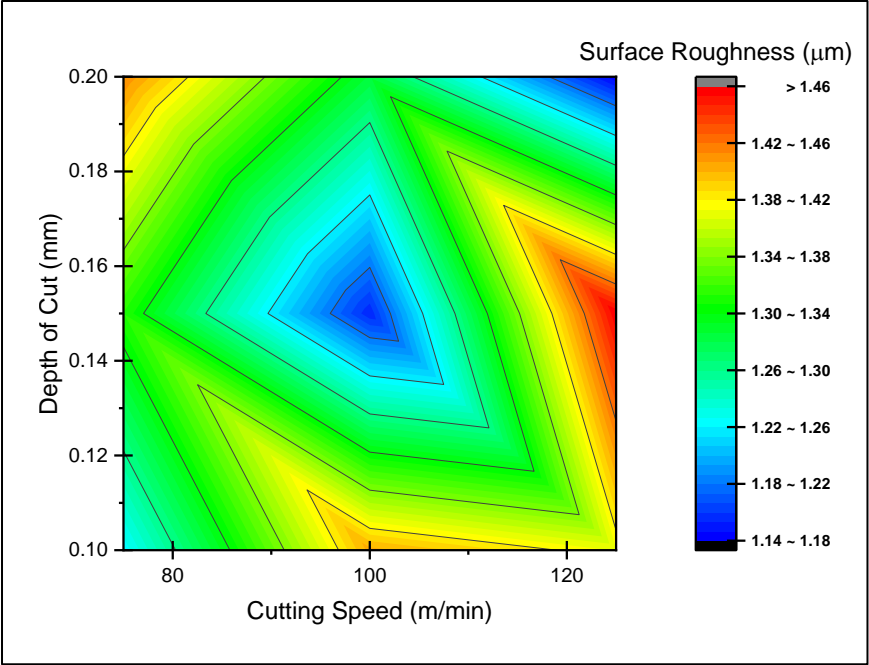


Figure 33: Contour plot for surface roughness: Cutting speed vs depth of cut (Uncoated Carbides)

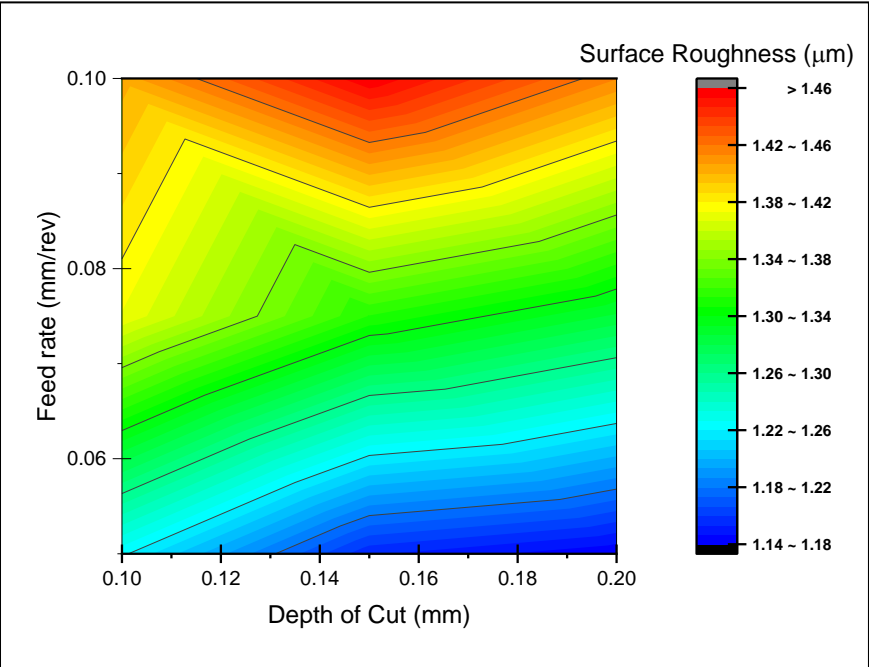


Figure 34: Contour plot for surface roughness: Feed rate vs depth of cut (Uncoated Carbides)

Response table for signal to noise (S/N) ratio of surface roughness has been shown in table 15. Main effect plots for signal to noise ratio of surface roughness has been shown in figure 35. It was observed that the highest S/N ratio obtained for surface roughness are cutting speed at 100 m/min, feed rate at 0.05 mm/rev and depth of cut at 0.2 mm. So, the optimal machining parameters for lower surface roughness were $v = 100 \text{ m/min}$, $f = 0.05 \text{ mm/rev}$, and $d = 0.2 \text{ mm}$ which can be represented as $v_2 - f_1 - d_3$. The corresponding level values for the parameters are bolded in table 15.

Table 15: Response table for signal to noise (S/N) ratio of surface roughness (Uncoated Carbides)

Symbol	Machining Parameters	S/N ratio			Max-Min	Rank
		Level 1	Level 2	Level 3		
v	Cutting speed (m/min)	-2.378	-2.129	-2.400	0.271	3
f	Feed rate (mm/rev)	-1.378	-2.440	-3.088	1.710	1
d	Depth of Cut (mm)	-2.485	-2.305	-2.116	0.369	2

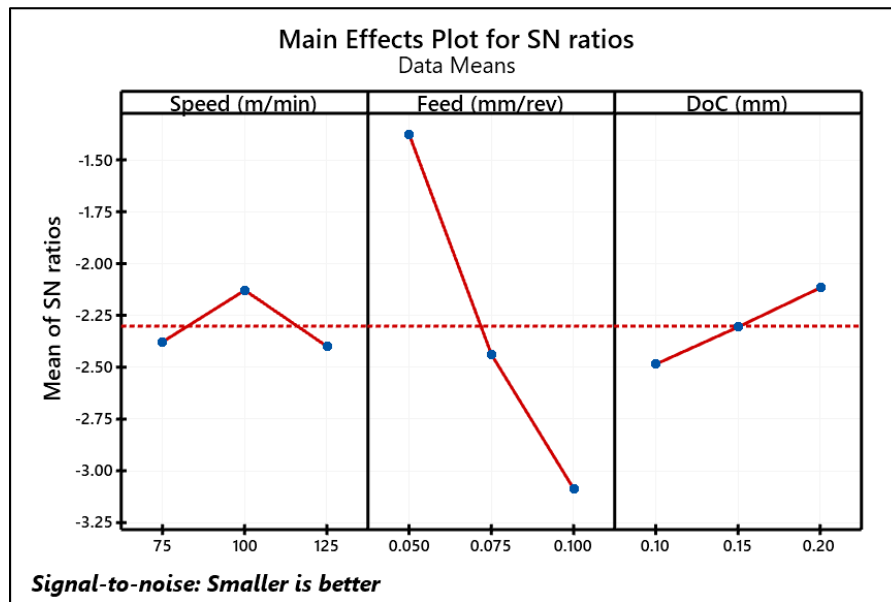


Figure 35: Main effect plots for S/N ratio of surface roughness (Uncoated Carbides)

Effects of Machining Parameters on Tool Wear Table 16 represents the response table for means of tool wear. It was observed that the machining parameter that influences the tool wear most is the cutting speed (Rank 1) followed by feed rate (Rank 2) and depth of cut (Rank 3). The effects of machining parameters on tool wear have been shown in figure 36. It was observed that tool wear increases with the increase of cutting speed. With the increase of cutting speed, the workpiece vibration and the friction in the cutting interface get increased leading to the increase of cutting zone temperature. As a result, the tool wear increases. It was observed that the tool wear increase with the increase of feed rate. Higher federate increases the material removal rate which increases the feed force, and the increased feed force increases the tool wear. With the increase of depth of cut tool wear increases. This is because higher depth of cut increases the cutting force as well as the contact area between workpiece and cutting tool which result in increased tool wear.

Table 16: Response table of means of tool wear (Uncoated Carbides)

Level	Means of Tool Wear (mm) for corresponding parameter level		
	Cutting Speed	Feed	DoC
1	0.4300	0.4263	0.4590
2	0.4463	0.4603	0.4563
3	0.4987	0.4883	0.4597
Delta	0.0687	0.0620	0.0033
Rank	1	2	3

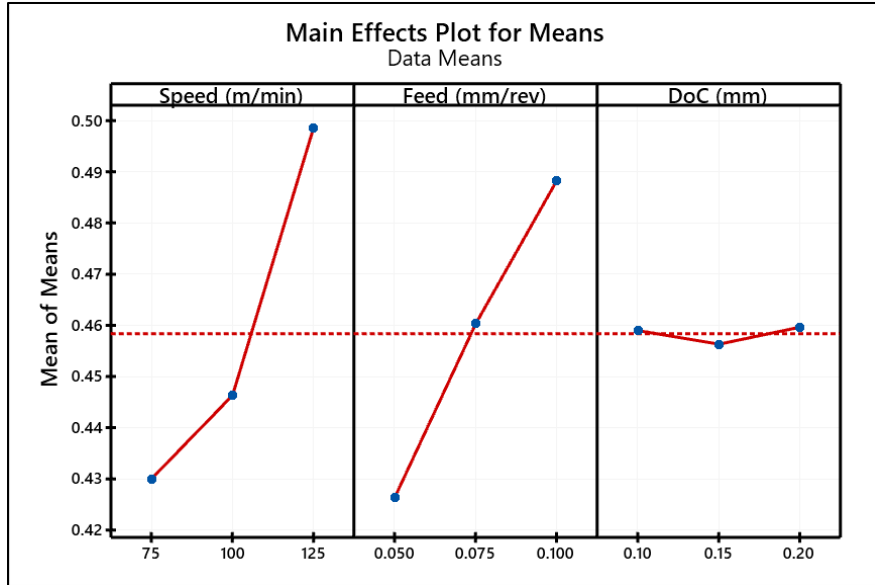


Figure 36: Effects of machining parameters on tool wear (Uncoated Carbides)

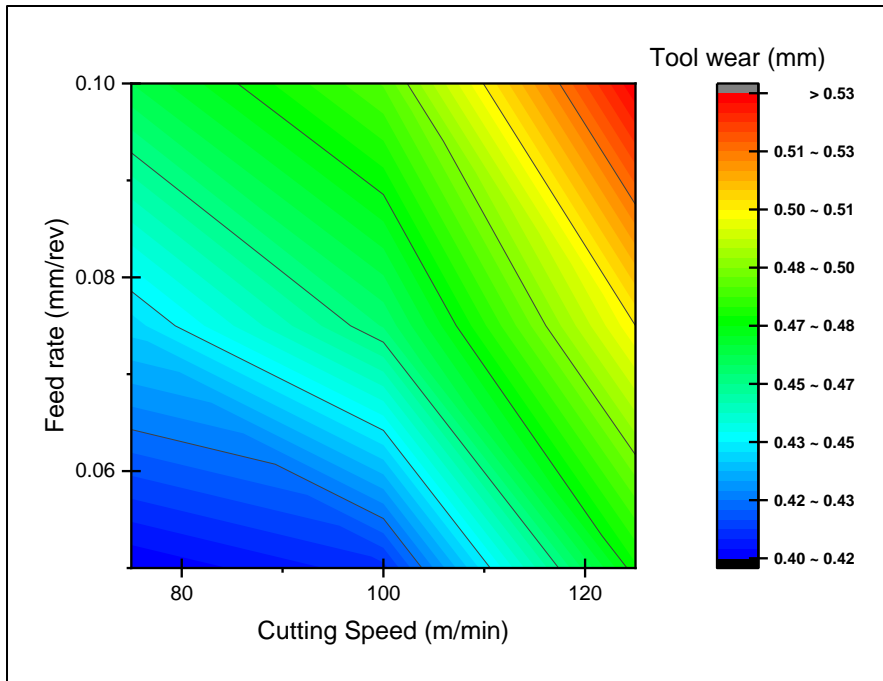


Figure 37: Contour plot for tool wear: Cutting speed vs feed rate (Uncoated Carbides)

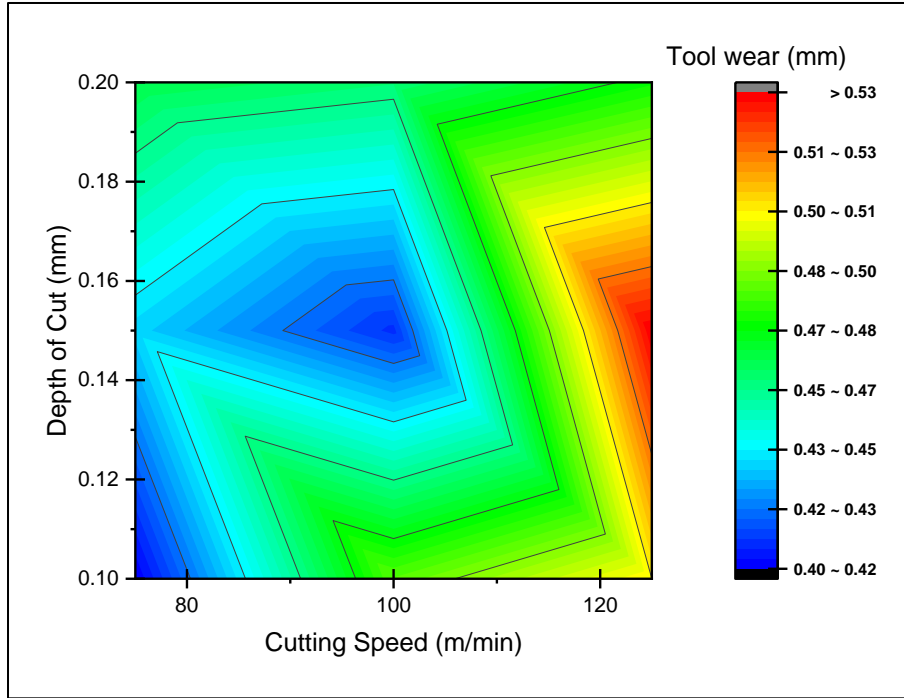


Figure 38: Contour plot for tool wear: Cutting speed vs depth of cut (Uncoated Carbides)

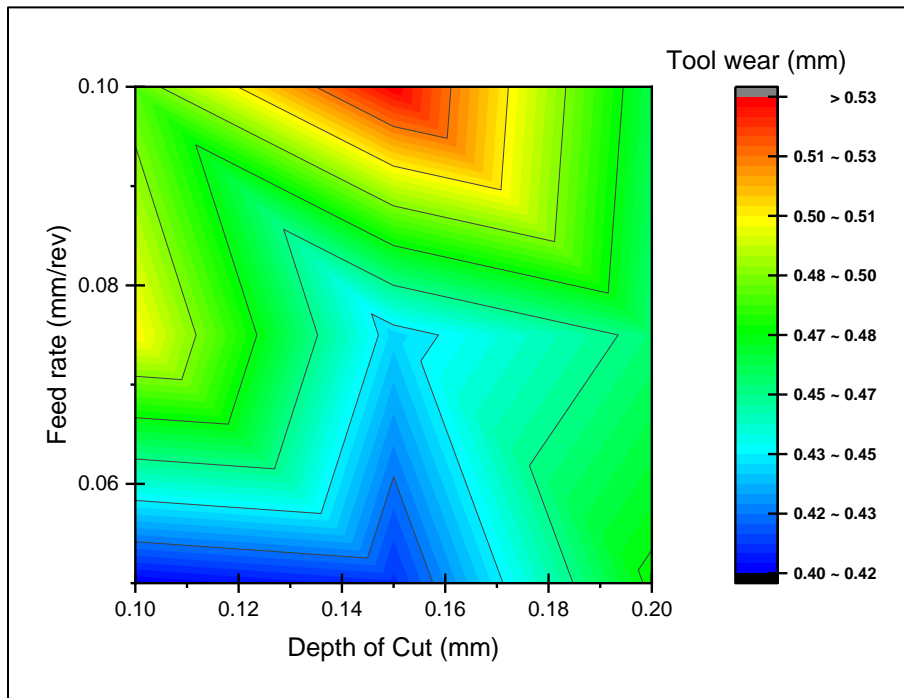


Figure 39: Contour plot for tool wear: Feed rate vs depth of cut (Uncoated Carbides)

Figure 37 explains the relation of tool wear with cutting speed and feed rate. It was observed that lower level of feed rate and cutting speed generates lower the tool wear. The lower left corner of the graph shows the lowest tool wear close to 0.40 mm that can be achieved using cutting speed around 70 m/min with feed rate near 0.05 mm/rev. Figure 38 indicates that depth of cut around 0.15 mm and cutting speed near 95 m/min can generate lower tool wear close to 0.41 mm. From figure 39, it is found that depth of cut between 0.1-0.15 mm and the feed rate near 0.05 mm/rev can be used to generate tool wear below 0.42 mm.

Response table for signal to noise (S/N) ratio of tool wear has been shown in table 17. Main effects plot of S/N ratio has been shown in figure 40. It was observed that the highest S/N ratio obtained for tool wear are cutting speed at 75 m/min, feed rate at 0.05 mm/rev and depth of cut at 0.15 mm. So, the optimal machining parameters for lower tool wear are $v = 75 \text{ m/min}$, $f = 0.05 \text{ mm/rev}$, and $d = 0.15 \text{ mm}$ which are represented as $v_1 - f_1 - d_2$. The corresponding level values of the parameters are bolded in table 17.

Table 17: Response table for signal to noise ratio (S/N) of tool wear (Uncoated Carbides)

Symbol	Machining Parameters	S/N ratio			Max-Min	Rank
		Level 1	Level 2	Level 3		
v	Cutting speed (m/min)	7.343	7.024	6.055	1.288	1
f	Feed rate (mm/rev)	7.425	6.755	6.242	1.183	2
d	Depth of Cut (mm)	6.800	6.870	6.752	0.118	3

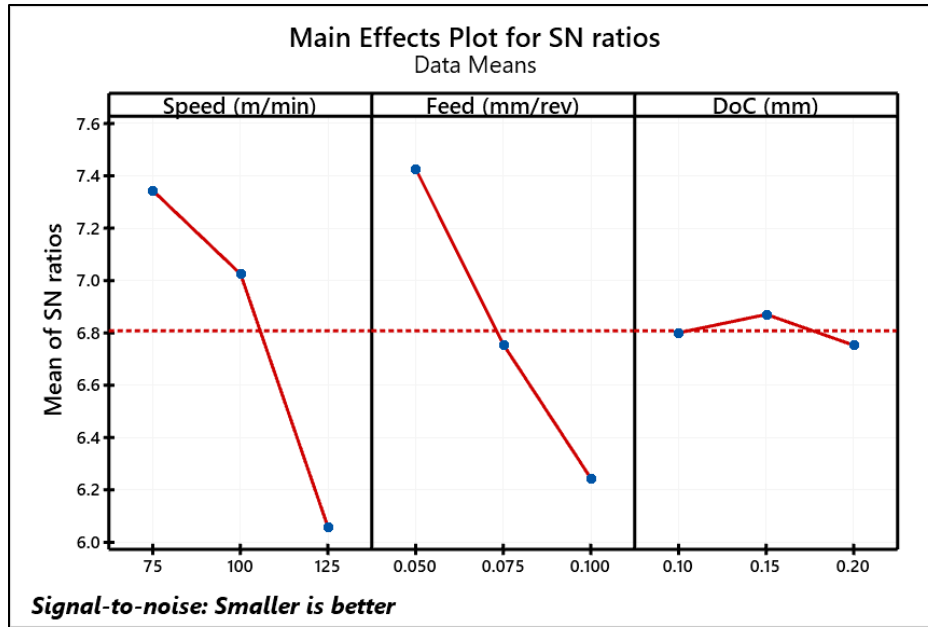


Figure 40: Main effects plot for S/N ratio of tool wear (Uncoated Carbides)

Linear Regression Model

Linear regression analysis was performed using Minitab 19 software to develop mathematical models for cutting force, tool wear and surface roughness as a function of cutting speed, feed rate and depth of cut. The efficiency of models was measured using a coefficient of determination R^2 which indicates how close the observed values are to the fitted regression line. The value of R^2 is represented on a scale of 0% to 100%. The higher the R^2 value, the better the regression model fits the observed data points. Normal probability plot of residuals (distance between the observed value and the fitted value) has been used to measure the significance of coefficients in the models. A straight line in the residual plot indicates that the observed values are close to the fitted values and the coefficients in the model are statistically significant.

Coated Carbides

It was observed that the R^2 values are very high for cutting force, tool wear and surface roughness models obtained from linear regression analysis. The normal probability plot of residuals for cutting force, surface roughness and tool wear have been shown in figure 41-43. It was observed from the figures that the residuals are very close to the fitted lines. So, it can be concluded that the coefficients in the models are significant.

$$\text{Cutting force } (F_c) = 10.66 - 0.0299 * v + 343.3 * f + 12.0 * d$$

$$(R^2 = 96.06\%; R^2(\text{adj}) = 93.93.70\%)$$

$$\text{Surface Roughness } (R_a) = 1.0291 + 0.000245 * v + 2.030 * f - 0.173 * d$$

$$R^2 = 93.37\% ; R^2(\text{adj}) = 89.39\%$$

$$\text{Tool wear} = 0.2027 + 0.000847 * v + 1.547 * f - 0.137 * d$$

$$R^2 = 93.87\%; R^2(\text{adj}) = 90.19\%$$

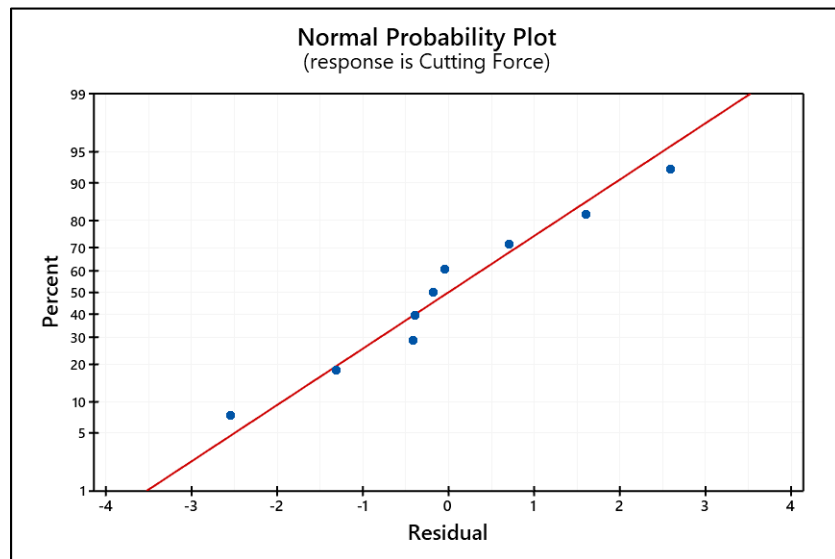


Figure 41: Normal probability plot of residuals for cutting force (Coated Carbides)

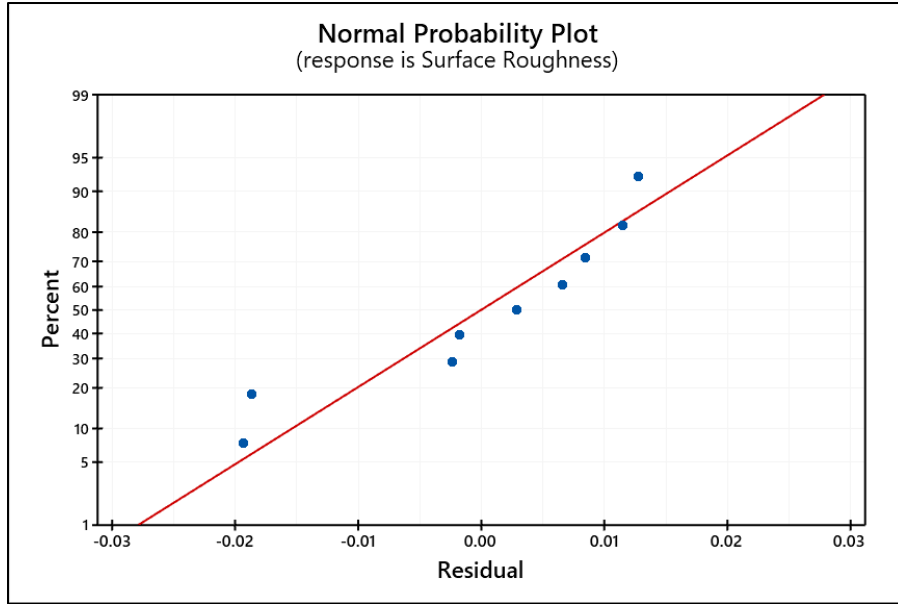


Figure 42: Normal probability plot of residuals for surface roughness (Coated Carbides)

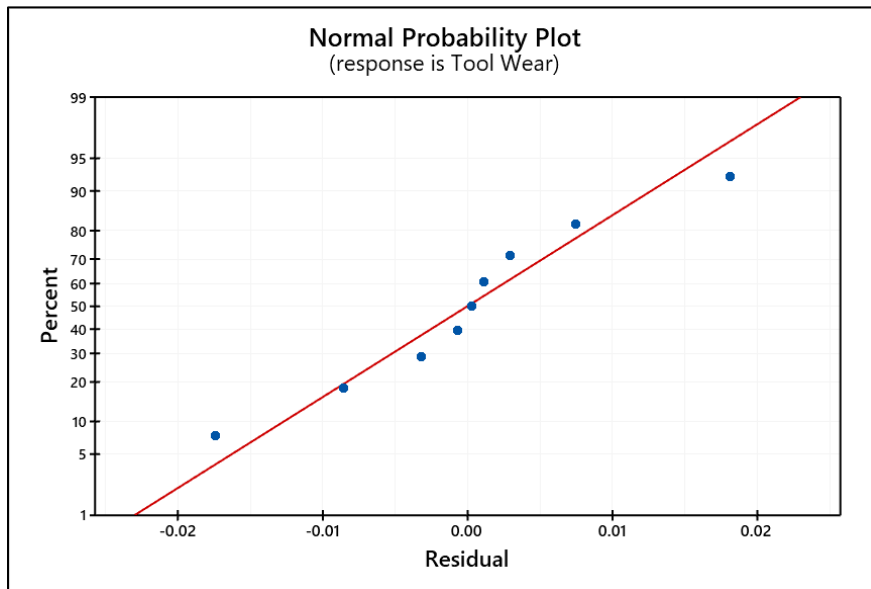


Figure 43: Normal probability plot of residuals for tool wear (Coated Carbides)

Uncoated Carbides

It was observed that the R^2 values are very high for cutting force, tool wear and surface roughness models obtained from linear regression analysis. The normal probability plot of residuals for cutting force, surface roughness and tool wear have been shown in figure 44-46. It was observed from the figures that the residuals are very close to the fitted lines. So, it can be concluded that the coefficients in the models are significant.

$$\text{Cutting Force } (F_c) = 10.59 - 0.0299 * v + 350.1 * f + 6.9 * d$$

$$R^2 = 97.17\%; R^2(\text{adj}) = 95.47\%$$

$$\text{Surface Roughness } (R_a) = 0.9891 + 0.000163 * v + 5.094 * f - 0.529 * d$$

$$R^2 = 93.87\%; R^2(\text{adj}) = 90.20\%$$

$$\text{Tool Wear} = 0.2230 + 0.001553 * v + 1.127 * f - 0.05 * d$$

$$R^2 = 95.65\%; R^2(\text{adj}) = 93.03\%$$

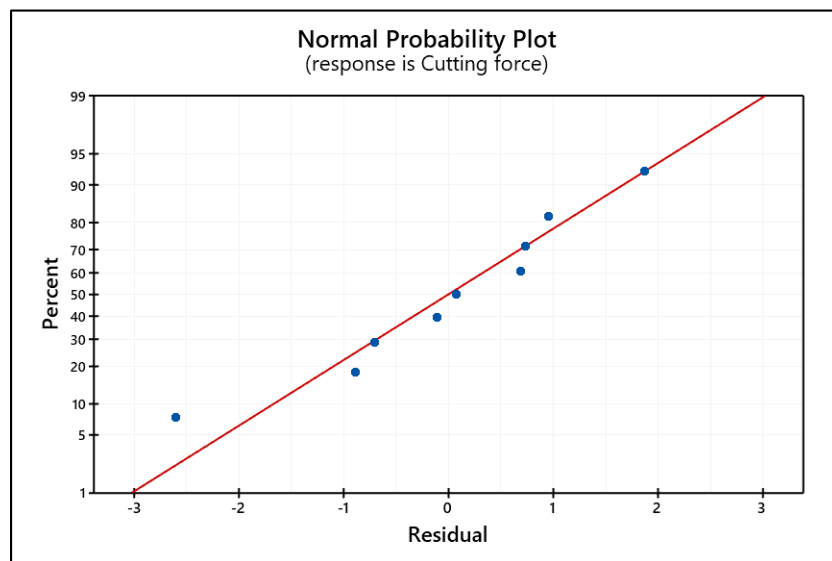


Figure 44: Normal probability plot of residuals for cutting force (Uncoated Carbides)

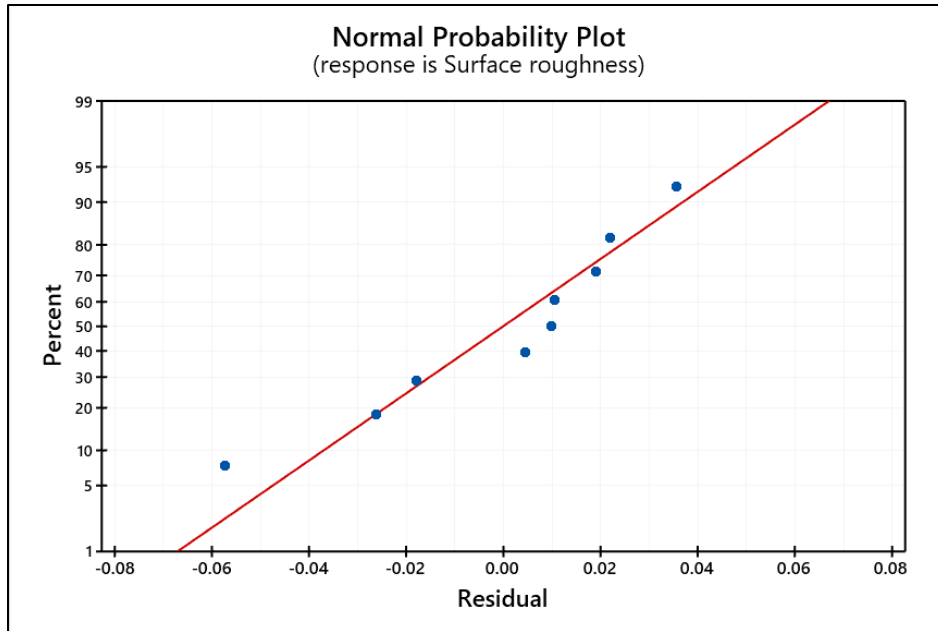


Figure 45: Normal probability plot of residuals for surface roughness (Uncoated Carbides)

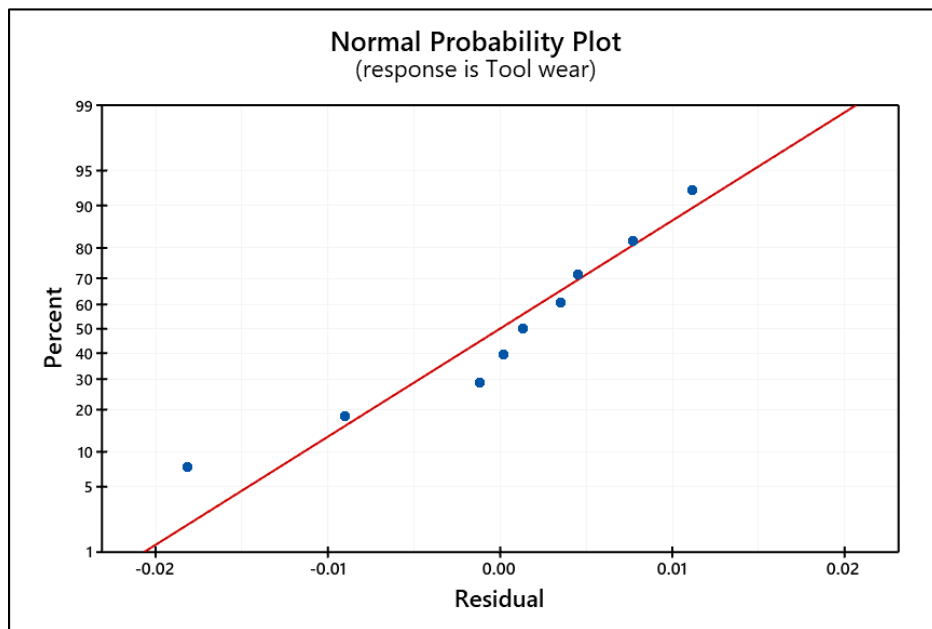


Figure 46: Normal probability plot of residuals for tool wear (Uncoated Carbides)

Multi-objective Optimization using Multi-Objective Genetic Algorithm (MOGA)

Multi-objective Genetic Algorithm (MOGA) was applied to perform the multi-objective optimization using Multi-objective GA solver in MATLAB 2020. This solver returns a set of non-dominated optimal solutions as outcomes of multi-objective optimization process which are called pareto optimal solutions or Paretian points. The Paretian points obtained from the optimization process were plotted in a graph and the knee point was selected as the optimal solution of the multi-objective optimization process. At first the multi-objective optimization was performed using two different objective functions such as cutting force-surface roughness, cutting force-tool wear, and surface roughness-tool wear. Then the multi-objective optimization was performed using three different objective functions- cutting force, tool wear and surface roughness. The goal of this study was to find the optimal combination of machining parameters to minimize the set of objective functions simultaneously. The following parameters were used in the optimization process while using GA:

Table 18: Parameters for GA

Parameter Name	Parameter Value
Population Size	50
Maximum no of generation	1000
Selection function	Tournament selection
Elite count	2
Crossover fraction	0.8
Crossover function	Constraint dependent
Mutation fraction	0.2
Mutation function	Constraint dependent
Number of parameters	3

Coated Carbide

Multi-Objective Optimization of Cutting Force and Surface Roughness Multi-Objective Genetic Algorithm (MOGA) was applied to minimize cutting force and surface roughness and the Paretian points obtained were shown in the table 19. Figure 47 shows the pareto front curve plotted using the Paretian points. It was observed that the point showing indices 12 indicates the knee point and it was selected as the optimal solution of multi-objective optimization of cutting force and surface roughness. The point represents the minimum cutting force of 27.22 N and surface roughness of 1.121 μm corresponding to the optimal level of cutting speed at 97.67 m/min, feed rate 0.05 mm/rev and depth of cut at 0.19 mm. The corresponding values has been bolded in table 19. The curve also shows several other optimal solutions which can be selected based on the choice of right parameters setting requirements for any condition.

Table 19: Paretian points obtained from multi-objective optimization of cutting force and surface roughness (Coated Carbides)

No.	Cutting Force (N)	Surface Roughness (μm)	Speed (m/min)	Feed (mm/rev)	DoC (mm)
1	25.37	1.143	124.86	0.05	0.10
2	25.39	1.143	124.29	0.05	0.10
3	25.52	1.141	123.86	0.05	0.11
4	25.66	1.140	118.79	0.05	0.11
5	25.74	1.139	118.45	0.05	0.12
6	25.92	1.136	117.40	0.05	0.13
7	26.34	1.131	115.63	0.05	0.16
8	26.39	1.130	114.71	0.05	0.17
9	26.48	1.129	115.44	0.05	0.17
10	26.89	1.126	99.45	0.05	0.17
11	27.07	1.123	101.82	0.05	0.19
12	27.22	1.121	97.67	0.05	0.19
13	27.40	1.121	90.27	0.05	0.19
14	27.47	1.119	92.26	0.05	0.20
15	27.81	1.116	79.96	0.05	0.20
16	27.98	1.114	75.00	0.05	0.20

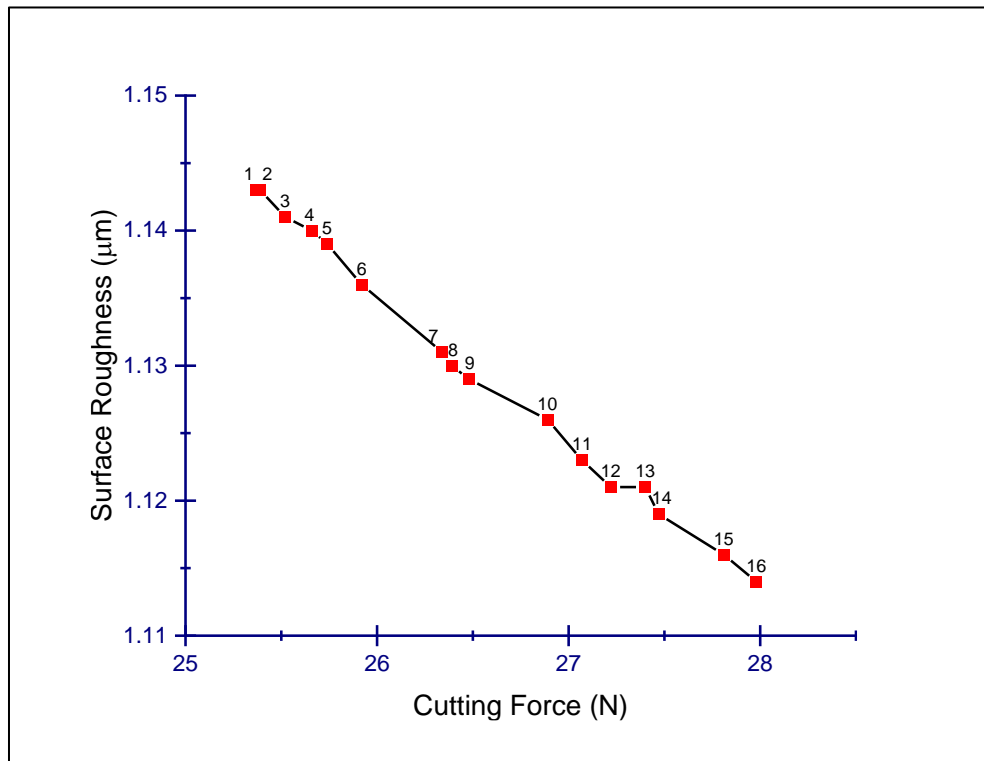


Figure 47: Pareto front of cutting force and surface roughness (Coated Carbides)

Multi-Objective Optimization of Cutting Force and Tool Wear Multi-objective optimization between cutting force and tool wear was performed using Genetic Algorithm and the Pareto points obtained were shown in the table 20. Figure 48 shows the Pareto front curve plotted using the Pareto points. It was observed that the point showing indices 11 indicates the knee points and it was selected as the optimal solution of multi-objective optimization of cutting force and tool wear. The point shows that the minimum cutting force value 27.13 N and the minimum tool wear value 0.327 mm can be obtained using the optimal parameter setting of cutting speed at 75.56 m/min, feed rate at 0.05 mm/rev and depth of cut at 0.13 mm. The corresponding values have been bolded in table 20. The curve also shows several other optimal

solutions which can be selected based on the choice of right parameters setting requirements for any condition.

Table 20: Paretian points obtained from multi-objective optimization of cutting force and tool wear (Coated Carbides)

No.	Cutting Force (N)	Tool wear (mm)	Speed (m/min)	Feed (mm/rev)	DoC (mm)
1	25.99	0.353	101.76	0.05	0.10
2	26.18	0.348	96.62	0.05	0.10
3	26.26	0.346	94.35	0.05	0.10
4	26.39	0.344	93.40	0.05	0.11
5	26.49	0.340	88.43	0.05	0.11
6	26.56	0.337	83.39	0.05	0.10
7	26.62	0.335	81.73	0.05	0.10
8	26.70	0.335	83.16	0.05	0.11
9	26.75	0.333	80.42	0.05	0.11
10	26.84	0.332	79.31	0.05	0.11
11	27.13	0.327	76.56	0.05	0.13
12	27.24	0.326	76.56	0.05	0.14
13	27.34	0.324	75.83	0.05	0.15
14	27.46	0.323	75.90	0.05	0.16
15	27.81	0.318	75.26	0.05	0.19
16	27.94	0.317	75.22	0.05	0.20

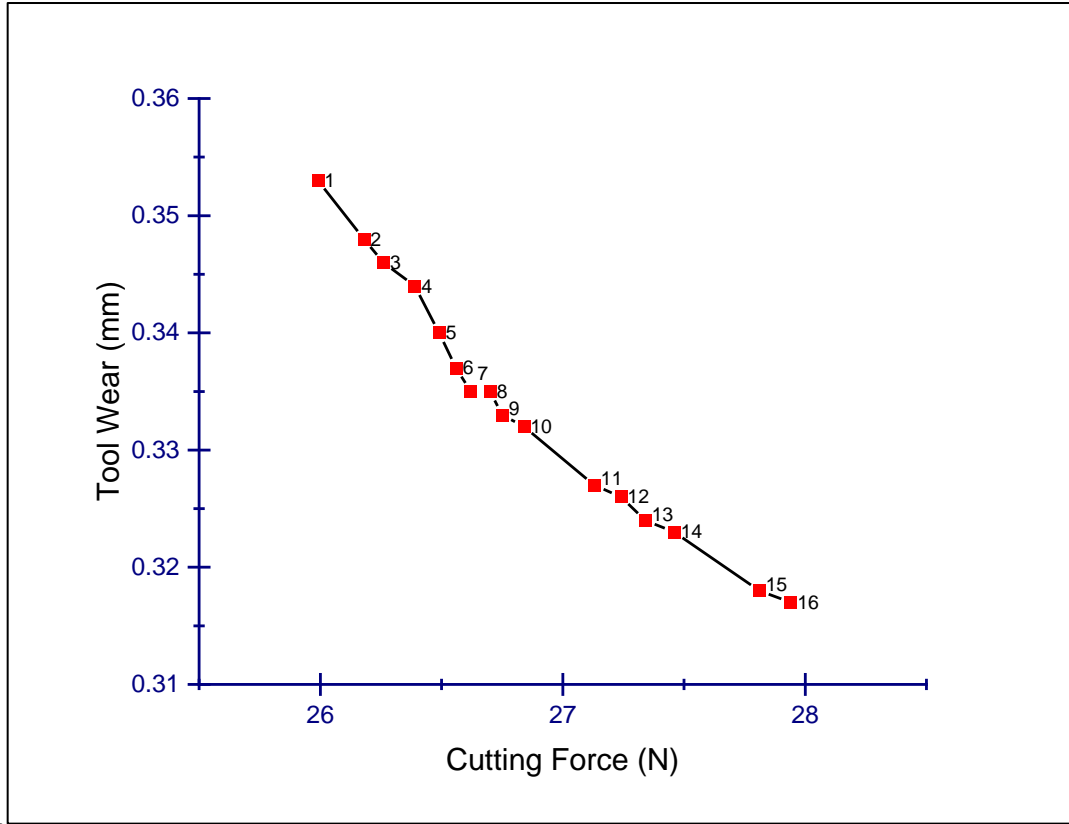


Figure 48: Pareto front of cutting force and tool wear (Coated Carbides)

Multi-Objective Optimization of Surface Roughness and Tool Wear Pareto optimal solution obtained from multi-objective optimization between surface roughness and tool wear was shown in the table 21. It was observed that the lowest surface roughness of 1.114 μm and tool wear of 0.316 mm were obtained at the optimal value of cutting speed at 75 m/min, feed rate at 0.05 mm/rev and depth of cut at 0.2 mm.

Table 21: Pareto optimal solution obtained from multi-objective optimization of surface roughness and tool wear (Coated Carbides)

Surface Roughness (μm)	Tool Wear (mm)	Speed (m/min)	Feed (mm/rev)	DoC (mm)
1.114	0.316	75	0.05	0.2

Multi-Objective Optimization of Cutting Force, Surface Roughness and Tool Wear

Table 22 shows the pareto optimal points obtained from the multi-objective optimization of cutting force, surface roughness and tool wear. Figure 49 shows the pareto front curve plotted using the pareto optimal points of table 22. It was observed that the point showing indices 11 indicates the knee point and it was selected as the optimal solution to the multi-objective optimization of cutting force, tool wear and surface roughness. The optimal solution provides minimum force of 27.21 N, minimum surface roughness of 1.121 μm and minimum tool wear of 0.336 mm at the optimal level of cutting parameters of cutting speed at 97.36 m/min, feed rate at 0.05 mm/rev and depth of cut at 0.19 mm. The curve also shows several other optimal solutions which can be selected based on the choice of right parameters setting requirements for any condition.

Table 22: Pareto optimal solution obtained from multi-objective optimization of cutting force, surface roughness and tool wear (Coated Carbides)

No.	Cutting Force (N)	Surface Roughness (μm)	Tool Wear (mm)	Speed (m/min)	Feed (mm/rev)	DoC (mm)
1	25.29	1.144	0.372	125.00	0.05	0.10
2	25.57	1.141	0.366	119.22	0.05	0.11
3	25.77	1.139	0.367	122.20	0.05	0.13
4	25.89	1.139	0.364	118.87	0.05	0.12
5	26.12	1.136	0.357	111.35	0.05	0.13
6	26.28	1.131	0.357	116.39	0.05	0.16
7	26.49	1.129	0.352	111.71	0.05	0.17
8	26.56	1.128	0.353	114.66	0.05	0.18
9	26.70	1.130	0.348	104.14	0.05	0.15
10	27.00	1.127	0.334	87.71	0.05	0.15
11	27.21	1.121	0.336	97.36	0.05	0.19
12	27.54	1.119	0.329	87.81	0.05	0.19
13	27.61	1.119	0.325	82.49	0.05	0.18
14	27.79	1.119	0.323	80.27	0.05	0.19
15	27.80	1.116	0.321	80.47	0.05	0.20
16	27.98	1.114	0.316	75.00	0.05	0.20

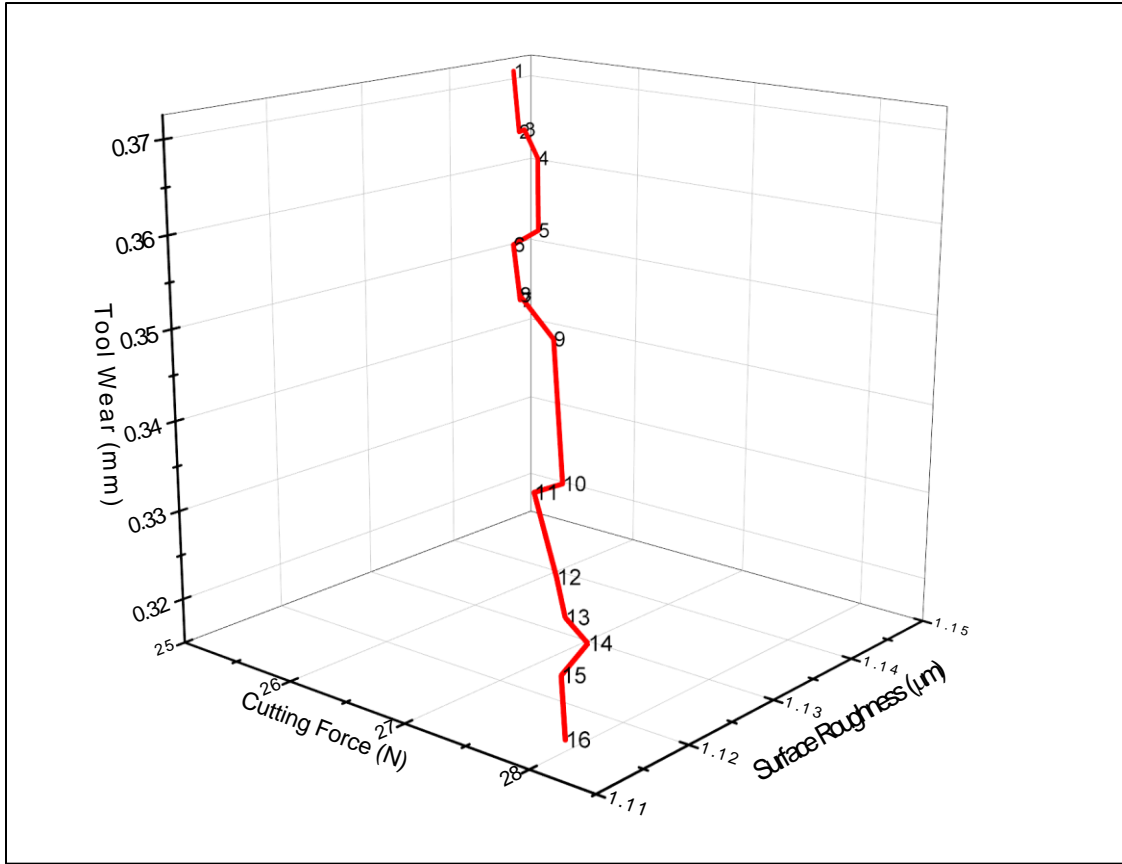


Figure 49: Pareto front of cutting force, surface roughness and tool wear (Coated Carbides)

Uncoated Carbide

Multi-Objective Optimization of Cutting Force and Surface Roughness Multi-Objective Genetic Algorithm (MOGA) was applied to minimize cutting force and surface roughness and the Pareto points obtained were shown in the table 23. Figure 50 shows the Pareto front curve plotted using the Pareto points. It was observed that the point showing indices 8 indicates the knee point and it was selected as the optimal solution of multi-objective optimization of cutting force and surface roughness. The point represents the minimum cutting force of 25.73 N and surface roughness of 1.160 µm corresponding to the optimal level of cutting speed at 124.57 m/min, feed rate 0.05 mm/rev and depth of cut at 0.20 mm. The

corresponding values has been bolded in table 23. The curve also shows several other optimal solutions which can be selected based on the choice of right parameters setting requirements for any condition.

Table 23: Pareto optimal solutions obtained from multi-objective optimization of cutting force and surface roughness (Uncoated Carbides)

No.	Cutting Force (N)	Surface Roughness (μm)	Speed (m/min)	Feed (mm/rev)	DoC (mm)
1	25.05	1.211	125.00	0.05	0.10
2	25.20	1.200	124.93	0.05	0.12
3	25.29	1.195	124.32	0.05	0.13
4	25.41	1.184	124.98	0.05	0.15
5	25.45	1.181	124.77	0.05	0.16
6	25.54	1.178	123.18	0.05	0.16
7	25.60	1.170	124.73	0.05	0.18
8	25.73	1.160	124.57	0.05	0.20
9	25.89	1.159	119.39	0.05	0.20
10	26.07	1.158	113.10	0.05	0.20
11	26.24	1.156	108.16	0.05	0.20
12	26.27	1.156	107.16	0.05	0.20
13	26.41	1.156	101.97	0.05	0.20
14	26.41	1.155	102.41	0.05	0.20
15	26.56	1.155	97.25	0.05	0.20
16	26.61	1.154	95.74	0.05	0.20

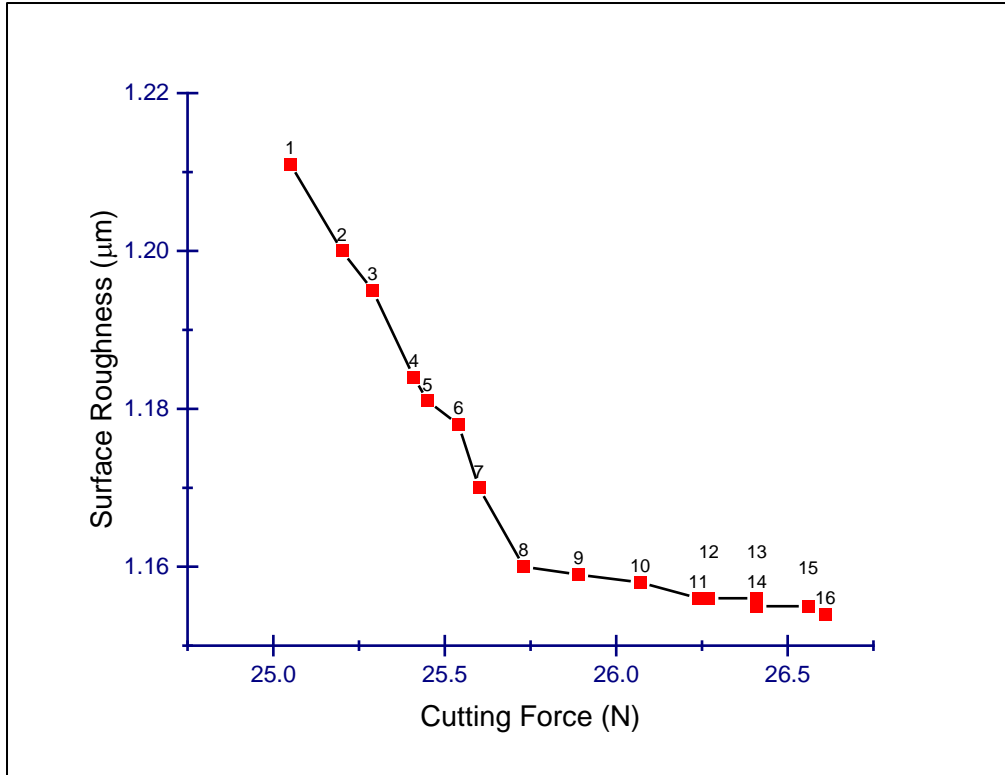


Figure 50: Pareto front of cutting force and surface roughness (Uncoated Carbides)

Multi-Objective Optimization of Cutting Force and Tool Wear Multi-objective optimization between cutting force and tool wear was performed using Genetic Algorithm and the Paretian points obtained were shown in the table 24. Figure 51 shows the pareto front curve plotted using the Paretian points. It was observed that the point showing indices 12 indicates the knee points and it was selected as the optimal solution of multi-objective optimization of cutting force and surface roughness. The point shows that the minimum cutting force value 26.42 N and the minimum tool wear value 0.402 mm can be obtained using the optimal parameter setting of cutting speed at 82.94 m/min, feed rate at 0.05 mm/rev and depth of cut at 0.11 mm. The corresponding values have been bolded in table 24. The curve also shows several other optimal solutions which can be selected based on the choice of right parameters setting requirements for any condition.

Table 24: Pareto optimal solutions obtained from multi-objective optimization of cutting force and tool wear (Uncoated Carbides)

No.	Cutting Force (N)	Tool wear (mm)	Speed (m/min)	Feed (mm/rev)	DoC (mm)
1	25.06	0.468	125.00	0.05	0.10
2	25.22	0.465	123.56	0.05	0.12
3	25.23	0.460	119.44	0.05	0.10
4	25.33	0.455	116.65	0.05	0.10
5	25.43	0.452	114.59	0.05	0.11
6	25.54	0.444	109.10	0.05	0.10
7	25.64	0.439	105.85	0.05	0.10
8	25.67	0.437	105.01	0.05	0.10
9	25.95	0.425	97.39	0.05	0.11
10	26.06	0.420	93.86	0.05	0.11
11	26.34	0.408	86.69	0.05	0.12
12	26.42	0.402	82.94	0.05	0.11
13	26.49	0.399	80.97	0.05	0.12
14	26.56	0.396	78.51	0.05	0.12
15	26.84	0.390	75.61	0.05	0.14
16	26.97	0.389	75.52	0.05	0.16
17	27.03	0.388	75.13	0.05	0.17
18	27.25	0.386	75.00	0.05	0.20

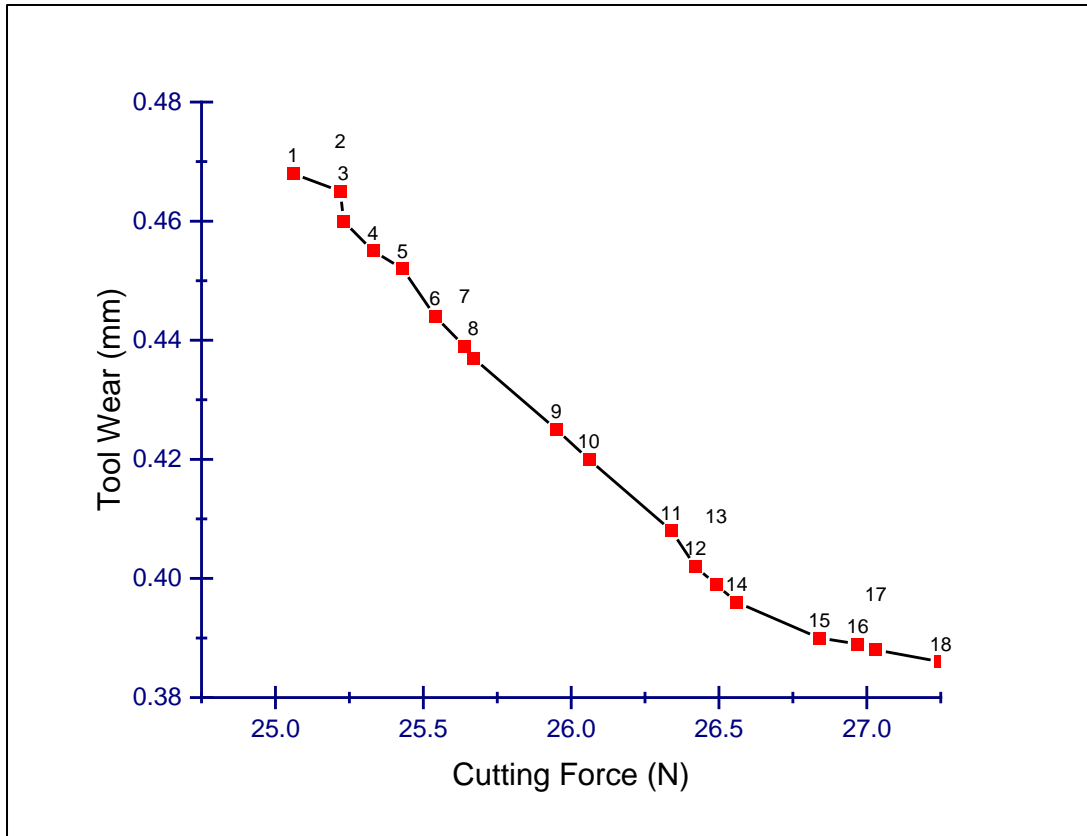


Figure 51: Pareto front of cutting force and tool wear (Uncoated Carbides)

Multi-Objective Optimization of Surface Roughness and Tool Wear Pareto optimal solution obtained from multi-objective optimization between surface roughness and tool wear was shown in the table 25. It was observed that the lowest surface roughness of 1.150 μm and tool wear of 0.386 mm were obtained at the optimal value of cutting speed at 75 m/min, feed rate at 0.05 mm/rev and depth of cut at 0.2 mm.

Table 25: Pareto optimal solution obtained from multi-objective optimization of surface roughness and tool wear (Uncoated Carbides)

Surface Roughness (μm)	Tool Wear (mm)	Speed (m/min)	Feed (mm/rev)	DoC (mm)
1.150	0.386	75.00	0.05	0.2

Multi-Objective Optimization of Cutting Force, Surface Roughness and Tool Wear

Table 26 shows the pareto optimal points obtained from the multi-objective optimization of cutting force, surface roughness and tool wear. Figure 52 shows the pareto front curve plotted using the pareto optimal points of table 26. It was observed that the point showing indices 9 indicates the knee point and it was selected as the optimal solution to the multi-objective optimization of cutting force, surface roughness and tool wear. The optimal solution provides minimum force of 26.59 N, minimum surface roughness of 1.1161 μm and minimum tool wear of 0.429 mm at the optimal level of cutting parameters of cutting speed at 102.42 m/min, feed rate at 0.05 mm/rev and depth of cut at 0.19 mm. The corresponding values have been bolded in table 26. Other pareto optimal solution can be selected based on the right parameter setting requirements of any condition.

Table 26: Pareto optimal solution obtained from multi-objective optimization of cutting force, surface roughness and tool wear (Uncoated Carbides)

No.	Cutting Force (N)	Surface Roughness (μm)	Tool Wear (mm)	Speed (m/min)	Feed (mm/rev)	DoC (mm)
1	27.25	1.150	0.386	75.00	0.05	0.20
2	27.13	1.159	0.389	76.44	0.05	0.19
3	27.04	1.155	0.396	81.01	0.05	0.19
4	26.92	1.168	0.403	85.09	0.05	0.17
5	26.35	1.184	0.416	92.47	0.05	0.14
6	26.62	1.163	0.419	95.51	0.05	0.18
7	26.26	1.178	0.425	98.47	0.05	0.16
8	26.13	1.188	0.431	101.70	0.05	0.14
9	26.59	1.161	0.429	102.42	0.05	0.19
10	26.47	1.162	0.434	105.41	0.05	0.19
11	25.75	1.195	0.444	110.21	0.05	0.13
12	25.65	1.191	0.457	118.44	0.05	0.14
13	25.33	1.200	0.462	121.65	0.05	0.12
14	25.16	1.208	0.465	123.09	0.05	0.11
15	25.08	1.211	0.468	124.70	0.05	0.10
16	25.07	1.211	0.469	125.00	0.05	0.10

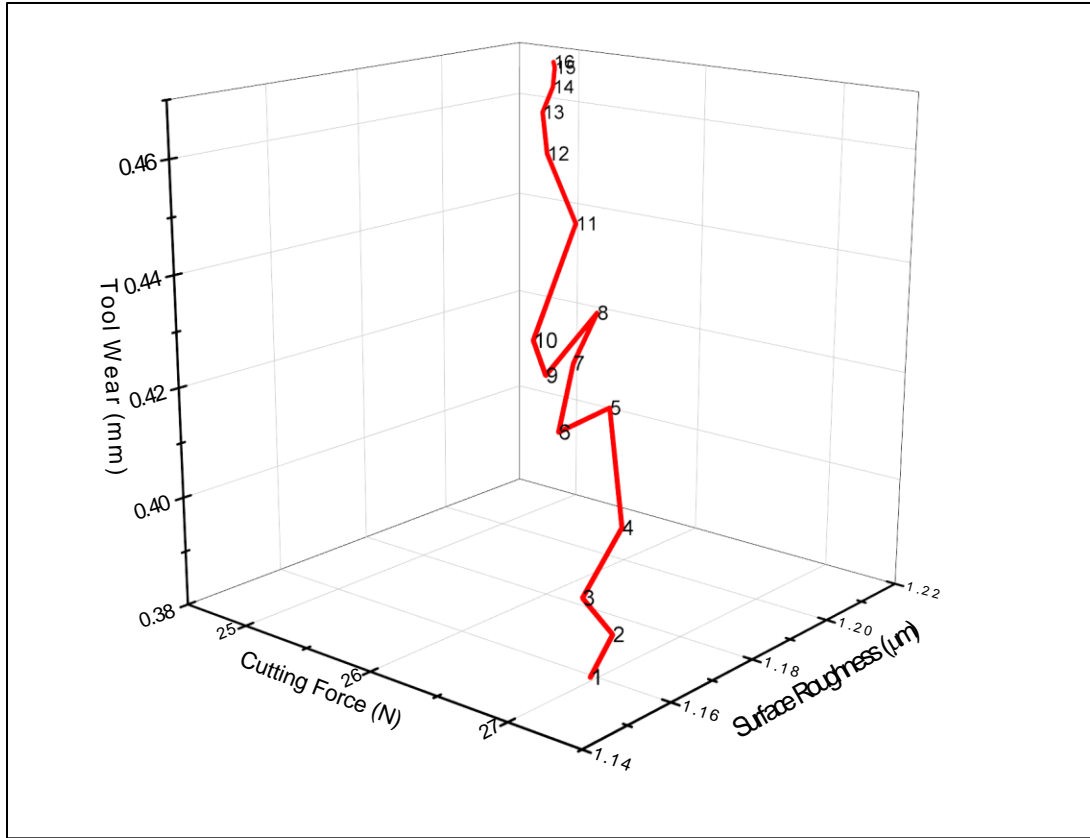


Figure 52: Pareto front of cutting force, surface roughness and tool wear (Uncoated Carbides)

Validation for Multi-Objective Optimization

Coated Carbide

Table 27: Validation experiment results for the optimal machining parameters using Coated Carbides

Response Characteristics	Cutting Parameters			Predicted			Experimental			Error (%)		
	v (m/min)	f (mm/rev)	d (mm)	F (N)	R_a (μm)	T (mm)	F (N)	R_a (μm)	T (mm)	F	R_a	T
Cutting Force, Surface Roughness	97.67	0.05	0.19	27.22	1.121		27.50	1.15		1.02	2.52	
Cutting Force, Tool Wear	75.56	0.05	0.13	27.13		0.327	27.81		0.336	2.44		2.68
Surface Roughness, Tool Wear	75	0.05	0.2		1.114	0.316		1.122	0.321		0.71	1.56
Cutting Force, Surface Roughness, Tool Wear	97.36	0.05	0.19	27.21	1.121	0.336	27.51	1.14	0.343	1.09	1.6	2.04

Uncoated Carbide

Table 28: Validation experiment results for the optimal machining parameters using uncoated carbides

Response Characteristics	Cutting Parameters			Predicted			Experimental			Error (%)		
	v (m/min)	f (mm/rev)	d (mm)	F (N)	Ra (μm)	T (mm)	F (N)	Ra (μm)	T (mm)	F	Ra	T
Cutting Force, Surface Roughness	124.57	0.05	0.20	25.73	1.16		26.20	1.14		1.79	-1.75	
Cutting Force, Tool Wear	82.94	0.05	0.11	26.42		0.402	27.13		0.410	2.61		1.95
Surface Roughness, Tool Wear	75	0.05	0.2		1.15	0.386		1.17	0.392		1.71	1.53
Cutting Force, Surface Roughness, Tool Wear	102.42	0.05	0.19	26.59	1.161	0.429	27.15	1.15	0.415	2.06	-0.96	-3.37

Comparative Study of the Machining Parameters between Coated and Uncoated Carbides

Effects of machining parameters on response characteristics have been studied comparatively between coated and uncoated carbide inserts based on Taguchi analysis. Figure 53 illustrates the effects of machining parameters on cutting force. It was observed that coated carbide inserts experience higher effects of cutting speed and depth of cut on cutting force compared to those of uncoated carbide inserts during turning of CFRP composites, but feed rate has almost similar effect for both coated and uncoated carbide inserts.

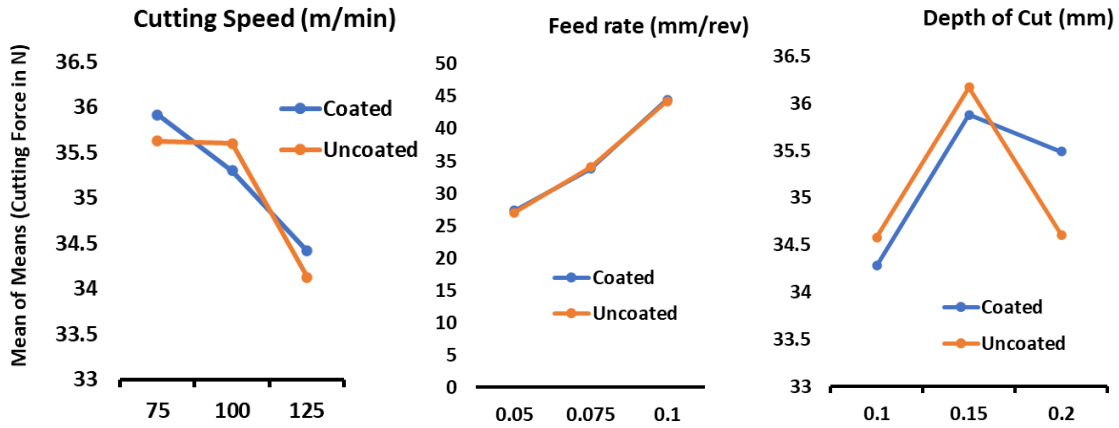


Figure 53: Comparative study on the effects of machining parameters on cutting force between coated and uncoated carbide inserts based on Taguchi Analysis

Figure 54 illustrates that effects of cutting speed, feed rate and depth of cut on surface roughness are always higher in coated carbide inserts compared to those of uncoated ones. Coated carbides always provide lower surface roughness compared to the uncoated carbides at any level of parameter settings.

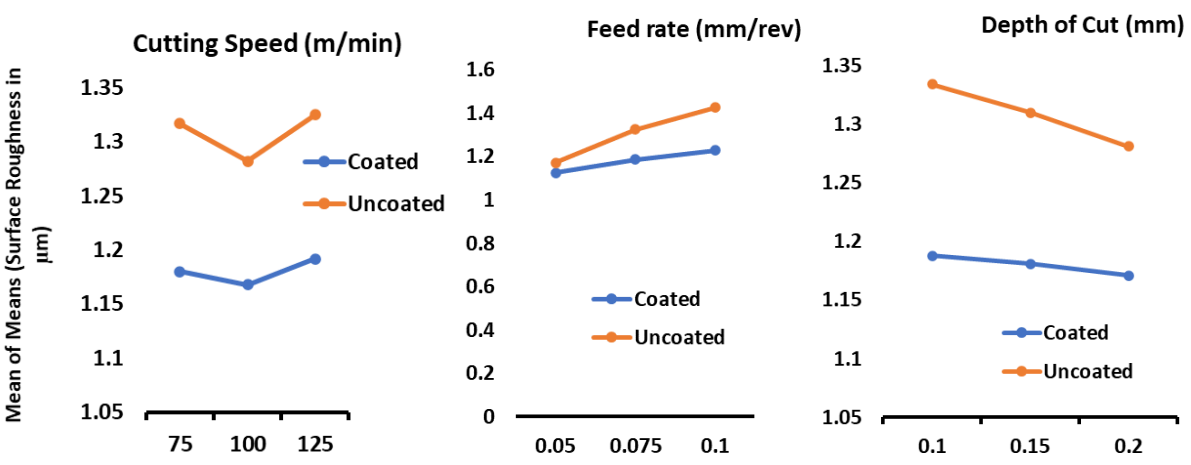


Figure 54: Comparative study on the effects of machining parameters on surface roughness between coated and uncoated carbide inserts based on Taguchi Analysis

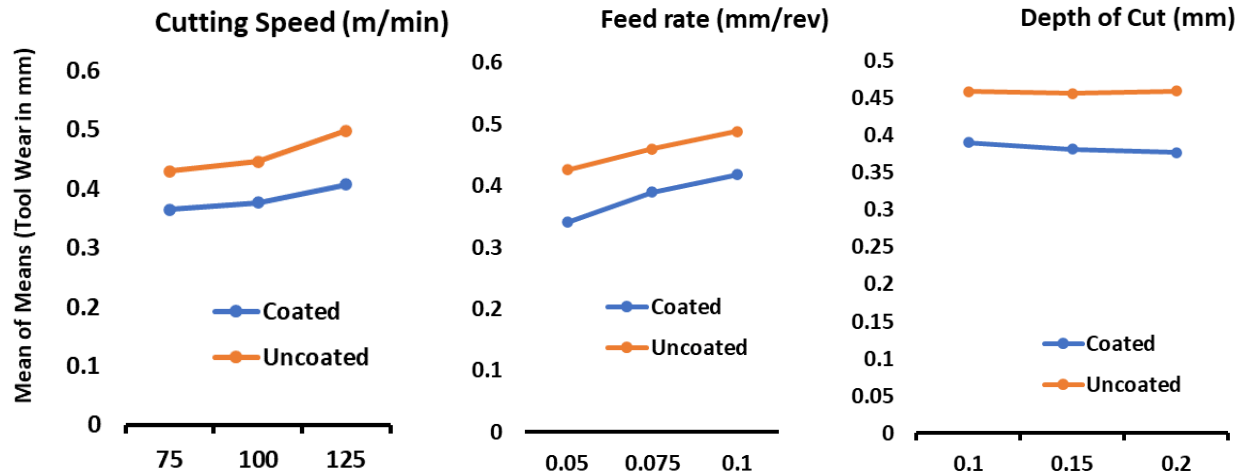


Figure 55: Comparative study on the effects of machining parameters on tool wear between coated and uncoated carbide inserts based on Taguchi Analysis

From figure 55, it was observed that uncoated carbides always have higher effects of cutting speed, feed rate and depth of cut on tool wear compared to those of coated carbides during turning of CFRP. Uncoated carbides always generate higher tool wear compared to the coated ones at any level of cutting parameter setting.

Table 27 shows the most significant machining parameters between coated and uncoated carbides for cutting force, surface roughness and tool wear. It was observed that feed has the most significant effects on cutting force and surface roughness for both coated and uncoated carbides. Tool wear is mostly affected by feed rate and cutting speed for coated and uncoated carbide respectively.

Table 29: Most significant machining parameters for coated and uncoated carbides

Response Characteristics	Most Significant Machining Parameters	
	Coated	Uncoated
Cutting Force	Feed	Feed
Surface Roughness	Feed	Feed
Tool Wear	Feed	Cutting Speed

Table 28 shows the optimal machining parameters for coated and uncoated carbide insert to minimize the corresponding response characteristics. It was observed that uncoated carbide insert uses higher cutting speed and depth of cut to provide lower cutting force, higher surface roughness and higher tool wear in optimized condition compared to those of coated carbide insert during turning of CFRP composites. This is due to the fact that uncoated carbide insert generates higher friction between workpiece and cutting tool on the machining surface during turning process which increases the cutting zone temperature. Due to the concentration of more heat on the cutting zone, the hardness of both workpiece and cutting tool gets decreased which leads to a decrease of cutting force and an increase of tool wear. Since the tool wear get increased, a higher cutting speed in optimum level is used to minimize this effect on surface roughness so that the surface roughness gets improved while keeping the tool wear at an optimal level corresponding to those machining parameters setting.

Table 30: Optimal machining parameters for coated and uncoated carbide inserts during turning of CFRP composites

Response Characteristics to be minimized	Type of Carbide Insert	Minimized values of Response Characteristics			Optimal Machining Parameters		
		Force (N)	Surface Roughness (μm)	Tool wear (mm)	Speed (m/min)	Feed (mm/rev)	Depth of Cut (mm)
Cutting Force and Surface Roughness	Coated	27.22	1.121		97.67	0.05	0.19
	Uncoated	25.73	1.160		124.57	0.05	0.20
Cutting Force and Tool wear	Coated	27.13		0.327	76.56	0.05	0.13
	Uncoated	26.42		0.402	82.94	0.05	0.11
Surface Roughness and Tool wear	Coated		1.114	0.316	75	0.05	0.2
	Uncoated		1.150	0.386	75.00	0.05	0.2
Cutting Force, Surface Roughness and Tool wear	Coated	27.21	1.121	0.336	97.36	0.05	0.19
	Uncoated	26.59	1.161	0.429	102.42	0.05	0.19

The optimization results reveal that lower cutting force is the only advantage of using uncoated carbide inserts over coated ones during turning of CFRP composite materials. However, the primary concern of the manufacturers is mostly the tool wear and surface roughness because these two are closely related to the production cost as well as the customer requirements. So, based on the comparative study between optimized conditions of coated and uncoated carbide inserts it was suggested that coated carbide insert is better in terms of improved surface roughness and lower tool wear compared to the uncoated carbide insert if the cutting force is not treated as a major concern. Figures 56-59 provide a better visualization of the comparative study on the optimized condition for coated and uncoated carbides.

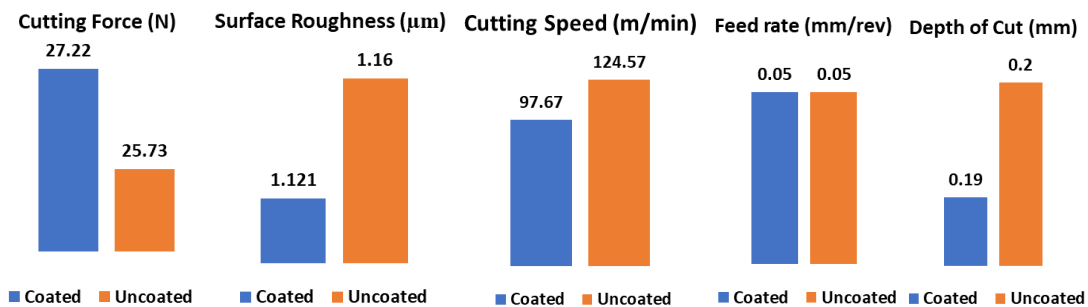


Figure 56: Comparative study on optimal parameters between coated and uncoated carbide inserts to minimize cutting force and surface roughness

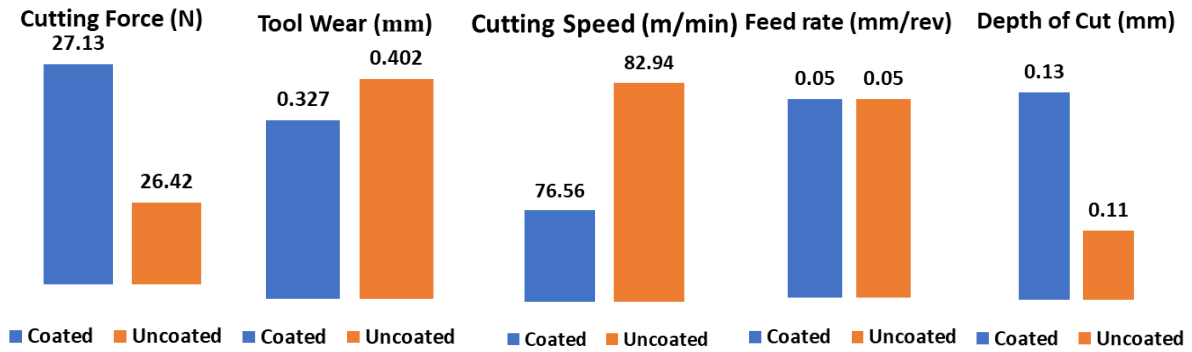


Figure 57: Comparative study on optimal parameters between coated and uncoated carbide inserts to minimize cutting force and tool wear

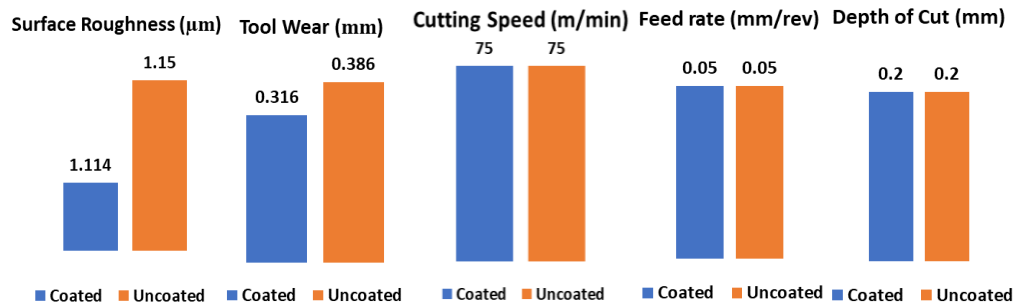


Figure 58: Comparative study on optimal parameters between coated and uncoated carbide inserts to minimize surface roughness and tool wear

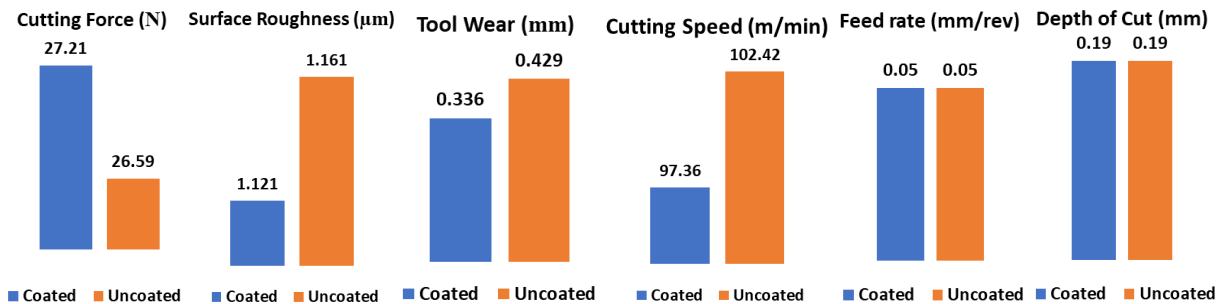


Figure 59: Comparative study on optimal parameters between coated and uncoated carbide inserts to minimize cutting force, surface roughness and tool wear

CHAPTER V

CONCLUSIONS

Turning operation of CFRP composites has been investigated using Taguchi Method, Regression Analysis and Multi-Objective Genetic Algorithm. It has been found that the most significant parameter during turning of CFRP composites is the feed rate followed by cutting speed and depth of cut. Coated carbide inserts provide lower surface roughness and tool wear, but higher cutting force compared to the those of uncoated carbides. The effects of machining parameters on response characteristics have been analyzed using S/N ratio analysis and contour plots. Lower feed rate along with higher cutting speed and higher depth of cut can generate lower surface roughness but can result in higher tool wear. Cutting Speed is very significant in tool wear for uncoated carbides.

The optimal parameter setting to minimize cutting force, surface roughness and tool wear using coated carbides includes cutting speed of 97.37 m/min, feed rate 0.05 mm/rev and depth of cut 0.19 mm. For uncoated carbides, these parameters include cutting speed of 102.42 m/min, feed rate 0.05 mm/rev and depth of cut 0.19 mm. The findings of this research complement the previous research in this field.

In the present work, the thermal effects of cutting zone temperature on tool wear and surface roughness have not been investigated. Also, the chip formation during turning of CFRP composites, the effect of chips getting attached to the machined surface due to high temperatures

and the effect of fiber delamination on tool wear and surface roughness have not been investigated and need to be investigated during turning of CFRP in future.

REFERENCES

- Abhishek, K., Datta, S., Chatterjee, S., & Mahapatra, S. S. (2014). Parametric optimization in turning of CFRP (epoxy) composites: A case experimental research with exploration of HS algorithm. *Applied Mechanics and Materials*,
- Abhishek, K., Datta, S., & Mahapatra, S. S. (2016). Multi-objective optimization in drilling of CFRP (polyester) composites: Application of a fuzzy embedded harmony search (HS) algorithm. *Measurement*, 77, 222-239.
- Abhishek, K., Datta, S., & Mahapatra, S. S. (2017). Optimization of MRR, surface roughness, and maximum tool-tip temperature during machining of CFRP composites. *Materials Today: Proceedings*, 4(2), 2761-2770.
- Abhishek, K., Datta, S., Masanta, M., & Mahapatra, S. S. (2017). Fuzzy embedded imperialist competitive algorithm (ICA) for multi-response optimization during machining of CFRP (Epoxy) composites. 2017 International conference on advances in mechanical, industrial, automation and management systems (AMIAMS),
- Abhishek, K., Kumar, V. R., Datta, S., & Mahapatra, S. S. (2017a). Application of JAYA algorithm for the optimization of machining performance characteristics during the turning of CFRP (epoxy) composites: comparison with TLBO, GA, and ICA. *Engineering with Computers*, 33(3), 457-475.
- Abhishek, K., Kumar, V. R., Datta, S., & Mahapatra, S. S. (2017b). Parametric appraisal and optimization in machining of CFRP composites by using TLBO (teaching-learning based optimization algorithm). *Journal of Intelligent Manufacturing*, 28(8), 1769-1785.
- Belmonte, M., Oliveira, F. J., Lanna, M., Silva, C., Corat, E. J., & Silva, R. F. (2004). Turning of CFRC composites using Si₃N₄ and thin CVD diamond coated Si₃N₄ tools. *Materials Science Forum*,
- Cao, Y., & Wu, Q. (1999). Teaching genetic algorithm using MATLAB. *International journal of electrical engineering education*, 36(2), 139-153.

- Chang, C. S. (2015). A Study of Cutting Temperatures in Turning Carbon-Fiber-Reinforced-Plastic (CRFP) Composites with Nose Radius Tools. *Key Engineering Materials*, 649, 38-45. <https://doi.org/10.4028/www.scientific.net/KEM.649.38>
- Chang, C. S., & Chang, Y. M. (2011). A Study of Cutting Temperatures in Turning Carbon-Fiber-Reinforced -Plastics (CFRP) Composites with Sharp Worn Tools. *Advanced Materials Research*, 233-235, 2790-2793. <https://doi.org/10.4028/www.scientific.net/AMR.233-235.2790>
- D'addona, D. M., & Teti, R. (2013). Genetic algorithm-based optimization of cutting parameters in turning processes. *Procedia Cirp*, 7, 323-328.
- Dandekar, C. R., & Shin, Y. C. (2012). Modeling of machining of composite materials: a review. *International Journal of Machine Tools and Manufacture*, 57, 102-121.
- Datta, R., & Majumder, A. (2010). Optimization of turning process parameters using multi-objective evolutionary algorithm. IEEE Congress on Evolutionary Computation,
- Davis, L. (1991). Handbook of genetic algorithms.
- Demir, Z., & Adiyaman, O. (2019). An investigation of the effect of tool approaching angle in turning of CFRP composite materials. *Materials Testing*, 61(11), 1109-1119. <https://doi.org/doi:10.3139/120.111429>
- Dureja, J., Gupta, V., Sharma, V. S., Dogra, M., & Bhatti, M. S. (2016). A review of empirical modeling techniques to optimize machining parameters for hard turning applications. *Proceedings of the Institution of Mechanical Engineers, Part B: Journal of Engineering Manufacture*, 230(3), 389-404.
- Ferreira, J., Coppini, N., & Neto, F. L. (2001). Characteristics of carbon-carbon composite turning. *Journal of Materials Processing Technology*, 109(1-2), 65-71.
- Ferreira, J., Coppini, N. L., & Miranda, G. (1999). Machining optimisation in carbon fibre reinforced composite materials. *Journal of Materials Processing Technology*, 92, 135-140.
- Ganesan, H., & Mohankumar, G. (2013). Optimization of machining techniques in CNC turning centre using genetic algorithm. *Arabian Journal for Science and Engineering*, 38(6), 1529-1538.
- Jain, R. K., & Jain, V. K. (2000). Optimum selection of machining conditions in abrasive flow machining using neural network. *Journal of Materials Processing Technology*, 108(1), 62-67.

- Kim, K. S., Kwak, Y. K., & Namgung, S. (1992). Machinability of carbon fiber-epoxy composite materials in turning. *Journal of Materials Processing Technology*, 32(3), 553-570.
- Kumar, K. V., & Sait, A. N. (2017). Modelling and optimisation of machining parameters for composite pipes using artificial neural network and genetic algorithm. *International Journal on Interactive Design and Manufacturing (IJIDeM)*, 11(2), 435-443.
- Mallick, P. K. (1993). Fiber-reinforced composites : materials, manufacturing, and design. <http://search.ebscohost.com/login.aspx?direct=true&scope=site&db=nlebk&db=nlabk&AN=12771>
- Pandey, H. M. (2016). Jaya a novel optimization algorithm: What, how and why? 2016 6th International Conference-Cloud System and Big Data Engineering (Confluence),
- Pandey, H. M. (2016, 14-15 Jan. 2016). Jaya a novel optimization algorithm: What, how and why? 2016 6th International Conference - Cloud System and Big Data Engineering (Confluence),
- Petkovic, D., & Radovanovic, M. (2013). Using genetic algorithms for optimization of turning machining process. *Journal of Engineering studies and research*, 19(1), 47.
- Rahman, M., Ramakrishna, S., Prakash, J., & Tan, D. (1999). Machinability study of carbon fiber reinforced composite. *Journal of Materials Processing Technology*, 89, 292-297.
- Rajasekaran, T., Gaitonde, V., & Davim, J. P. (2013). Fuzzy modeling and analysis on the turning parameters for machining force and specific cutting pressure in CFRP composites. *Materials Science Forum*,
- Rajasekaran, T., Palanikumar, K., & Arunachalam, S. (2013). Investigation on the turning parameters for surface roughness using Taguchi analysis. *Procedia Engineering*, 51, 781-790.
- Rajasekaran, T., Palanikumar, K., & Vinayagam, B. (2012a). Experimental investigation and analysis in turning of CFRP composites. *Journal of Composite Materials*, 46(7), 809-821.
- Rajasekaran, T., Palanikumar, K., & Vinayagam, B. (2012b). Turning CFRP composites with ceramic tool for surface roughness analysis. *Procedia Engineering*, 38, 2922-2929.
- Rao, R. V., & Patel, V. (2013, 2013/06/01/). An improved teaching-learning-based optimization algorithm for solving unconstrained optimization problems. *Scientia Iranica*, 20(3), 710-720. <https://doi.org/https://doi.org/10.1016/j.scient.2012.12.005>
- Rao, R. V., Savsani, V. J., & Balic, J. (2012, 2012/12/01). Teaching-learning-based optimization algorithm for unconstrained and constrained real-parameter optimization problems.

Engineering Optimization, 44(12), 1447-1462.
<https://doi.org/10.1080/0305215X.2011.652103>

Roy, Y. A., Gobivel, K., Sekar, K. V., & Kumar, S. S. High Speed Turning of Carbon Fiber–Epoxy Composite Material.

Saravanakumar, K., Kumar, M. R., & ShaikDawood, D. A. (2012). Optimization of CNC turning process parameters on Inconel 718 using genetic algorithm. *IRACST–Engineering Science and Technology: An International Journal (ESTIJ)*, 2(4).

Sardinas, R. Q., Santana, M. R., & Brindis, E. A. (2006). Genetic algorithm-based multi-objective optimization of cutting parameters in turning processes. *Engineering Applications of Artificial Intelligence*, 19(2), 127-133.

Sasahara, H., Kikuma, T., Koyasu, R., & Yao, Y. (2014). Surface grinding of carbon fiber reinforced plastic (CFRP) with an internal coolant supplied through grinding wheel. *Precision Engineering*, 38(4), 775-782.

Sauer, K., Hertel, M., Fickert, S., Witt, M., & Putz, M. (2020). Cutting parameter study of CFRP machining by turning and turn-milling. *Procedia Cirp*, 88, 457-461.

Savage, E. (2012). *Carbon-carbon composites*. Springer Science & Business Media.

Sönmez, A. İ., Baykasoğlu, A., Dereli, T., & Fıfız, İ. H. (1999). Dynamic optimization of multipass milling operations via geometric programming. *International Journal of Machine Tools and Manufacture*, 39(2), 297-320.

Soo, S. L., Shyha, I. S., Barnett, T., Aspinwall, D. K., & Sim, W.-M. (2012). Grinding performance and workpiece integrity when superabrasive edge routing carbon fibre reinforced plastic (CFRP) composites. *CIRP annals*, 61(1), 295-298.

BIOGRAPHICAL SKETCH

S M Abdur Rob obtained Bachelor of Science in Industrial and Production engineering from Bangladesh University of Engineering and Technology in 2018 and joined the Department of Manufacturing and Industrial Engineering at the University of Texas Rio Grande Valley in Spring 2020. He worked as a research assistant at the Advanced Machining Laboratory under the supervision of Dr. Anil K. Srivastava and completed his Master of Science in Manufacturing Engineering in August 2021. His research interests are focused on Advanced Machining, Design and Manufacturing, Thermodynamics & Heat Transfer, Fluid Mechanics, and Additive Manufacturing. During his master's study, he was awarded the Presidential Graduate Research Assistantship award. He has published one article in a prestigious journal and is currently working on two more articles. He is joining Groove School of Engineering at The City College of New York to pursue his PhD in Mechanical Engineering in Fall 2021. He can be reached at abdurrob.buet@gmail.com.